



Minerva Access is the Institutional Repository of The University of Melbourne

Author/s:

Phillips, D;Matchan, EL;Dalton, H;Kuiper, KF

Title:

Revised astronomically calibrated $40\text{Ar}/39\text{Ar}$ ages for the Fish Canyon Tuff sanidine - Closing the interlaboratory gap

Date:

2022-05-20

Citation:

Phillips, D., Matchan, E. L., Dalton, H. & Kuiper, K. F. (2022). Revised astronomically calibrated $40\text{Ar}/39\text{Ar}$ ages for the Fish Canyon Tuff sanidine - Closing the interlaboratory gap. *Chemical Geology*, 597, <https://doi.org/10.1016/j.chemgeo.2022.120815>.

Persistent Link:

<https://hdl.handle.net/11343/330130>

Chemical Geology

Revised astronomically calibrated $^{40}\text{Ar}/^{39}\text{Ar}$ ages for the Fish Canyon Tuff sanidine - Closing the interlaboratory gap --Manuscript Draft--

Manuscript Number:	CHEMGE14568R2
Article Type:	Research paper
Keywords:	$^{40}\text{Ar}/^{39}\text{Ar}$ geochronology; reference minerals, Fish Canyon Tuff; Alder Creek Rhyolite, Mount Dromedary
Corresponding Author:	David Phillips, PhD The University of Melbourne Parkville, VIC AUSTRALIA
First Author:	David Phillips, PhD
Order of Authors:	David Phillips, PhD Erin L Matchan Hayden Dalton Klaudia F Kuiper
Abstract:	<p>The $^{40}\text{Ar}/^{39}\text{Ar}$ geochronology method is capable of high precision (<0.05%), but remains limited by relatively large uncertainties in ^{40}K decay constants and the ages of natural reference mineral standards. The most widely used $^{40}\text{Ar}/^{39}\text{Ar}$ reference mineral is the well-known ca. 28 Ma Fish Canyon Tuff sanidine (FCTs). Several studies have attempted to calibrate FCTs against astronomically tuned tephra in Crete (Faneromeni A1 tephra) and Morocco (Messâdit Mes4 tuff) as well as deep-sea sedimentary sequences. Previously reported astronomically tuned ages range from 28.126 ± 0.019 to 28.21 ± 0.18 Ma (2s), a range of ~0.3%, compared to precision levels of <0.05% achievable by new generation, multi-collector mass spectrometer systems.</p> <p>In this study, we revisit the astronomical calibration of FCTs. Relative to ages of 6.943 ± 0.005 Ma for A1 tuff sanidine (A1Ts) and 6.791 ± 0.010 Ma (2s) for Mes4 tuff sanidine (Mes4Ts), we calculate revised astronomically tuned ages for Fish Canyon Tuff sanidine of 28.175 ± 0.012 Ma (± 0.023 Ma, including the uncertainty in the age of A1Ts) and 28.176 ± 0.010 Ma (± 0.042 Ma, including the uncertainty in the age of Mes4Ts), respectively (assuming negligible differential ^{39}Ar recoil loss). This age is within uncertainty of most recent astronomical intercalibrations, permitting calculation of inter-laboratory mean ages of 28.176 ± 0.010 (± 0.023) Ma and 28.179 ± 0.009 (± 0.042) Ma, respectively. As the astronomical age of the A1 Tuff is more precise than that of the Mes4 Tuff, we recommend the former value is adopted as the astronomical age for FCTs. This age is consistent with available U-Pb zircon age data, but remains distinctly older than recent astronomical ages of 28.10 and 28.150 Ma inferred from deep-sea Ocean Drilling Program sediments, indicating that further work is required to align the astronomical tuning of terrestrial versus deep-sea sediments.</p> <p>Based on previous R-values for the Alder Creek Rhyolite sanidine (ACRs) and Mount Dromedary biotite (MD-2b) reference minerals, co-irradiated with FCTs, we calculate revised astronomically calibrated ages of 1.18342 ± 0.00069 (± 0.0090) Ma for ACRs and 99.323 ± 0.077 (± 0.33) Ma for MD-2b, the latter amended to 99.20 ± 0.11 (± 0.38) Ma to account for relative recoil loss of ^{39}Ar K.</p>

CHEMGE14568

Response to Editor Comments

The Editor requested two minor changes to the manuscript:

- 1) “include a statement in the abstract (e.g. after current line 35) explaining that when reference materials are characterised with the level of precision of your study, other factors, such as differential recoil (see your lines 271-273), need to be controlled with even greater care so as to avoid producing data that are more precise than accurate.”

We have added a sentence at the end of the abstract that addresses this issue (lines 39-41 of the revised manuscript).

- 2) “Secondly, I remain a bit puzzled by your insistence that the populations of separated/analysed feldspars from these reference materials could be expected to be completely homogeneous. I was struck by this on two occasions in the m/s. Firstly, on lines 223-232, you discuss the $MSWD > 1$, which you attribute, in order, to: blank 'aberrations', variations in neutron flux gradients, or excess argon (a geological factor). While I agree that antecrysts and xenocrysts can be dismissed, I'm reminded of the work of petrologists and geochemists on crystal cargo in volcanic products. That work clearly informs that prior to eruption, cargo crystals are typically sourced from different locations within the complex magma conduits. I would have thought that the geological explanation (i.e. the crystals collectively recording a history on the order of an apparent 10,000 Ar/Ar years) would be the most straight forward. The second place where I was reminded is when you discuss the apparent Ca/K ratio variations. I agree that with the exception of the 2 clearly elevated Ca/K crystals, the variability in Ca/K is not large, however, it is several tens if not $> 100\%$. I think it would be prudent, at that point, to refer to the fact that the FCT does contain megacrysts with much greater Ca/K variability and that this variability, although not uniquely responsible for the $MSWD$ dispersion > 1 , could be a real petrological phenomenon of the magma that was tapped for the FCT.”

We think that there may be a misunderstanding in this case. We agree that felsic magmas entrain a variably heterogeneous crystal cargo. Our contention is that the ages of sanidine crystals from the three tuffs is homogeneous, with some caveats. As the closure temperature for argon diffusion in feldspars is relatively low, most entrained feldspar crystals would be expected to be reset to the time of magma eruption and inheritance should be rare. Nonetheless, we concede that the slightly elevated $MSWD$ values for many sanidine aliquots may be attributable to a number of causes, including inherited and excess argon. Therefore, we have revised lines 221 to 224 and 229 to 235 to make these points.

- Fish Canyon Tuff sanidine calibrated against astronomically tuned A1 and Mes4 tuffs
- Revised inter-laboratory astronomical $^{40}\text{Ar}/^{39}\text{Ar}$ age for Fish Canyon Tuff sanidine
- Astronomically calibrated ages for Alder Creek Rhyolite and Mount Dromedary standards

1 Revised astronomically calibrated $^{40}\text{Ar}/^{39}\text{Ar}$ ages for the Fish
2 Canyon Tuff sanidine – closing the interlaboratory gap

3

4 D. Phillips^{a*}, E.L. Matchan^a, H. Dalton^a and Kuiper, K.F.^b

5 *^aSchool of Geography, Earth and Atmospheric Sciences, The University of Melbourne,
6 Parkville, VIC, 3010, Australia.*

7 *^bFaculty of Earth and Life Sciences, Vrije Universiteit Amsterdam, The Netherlands.*

8

9 **Corresponding author; E-mail: dphillip@unimelb.edu.au*

10

11 **Abstract**

12

13 The $^{40}\text{Ar}/^{39}\text{Ar}$ geochronology method is capable of high precision (<0.05%), but remains
14 limited by relatively large uncertainties in ^{40}K decay constants and the ages of natural
15 reference mineral standards. The most widely used $^{40}\text{Ar}/^{39}\text{Ar}$ reference mineral is the well-
16 known ca. 28 Ma Fish Canyon Tuff sanidine (FCTs). Several studies have attempted to
17 calibrate FCTs against astronomically tuned tephra in Crete (Faneromeni A1 tephra) and
18 Morocco (Messâdit Mes4 tuff) as well as deep-sea sedimentary sequences. Previously
19 reported astronomically tuned ages range from 28.126 ± 0.019 to 28.21 ± 0.18 Ma (2σ), a
20 range of ~0.3%, compared to precision levels of <0.05% achievable by new generation,
21 multi-collector mass spectrometer systems. In this study, we revisit the astronomical
22 calibration of FCTs. Relative to ages of 6.943 ± 0.005 Ma for A1 tuff sanidine (A1Ts) and
23 6.791 ± 0.010 Ma (2σ) for Mes4 tuff sanidine (Mes4Ts), we calculate revised
24 astronomically tuned ages for Fish Canyon Tuff sanidine of 28.175 ± 0.012 Ma (± 0.023

25 Ma, including the uncertainty in the age of A1Ts) and 28.176 ± 0.010 Ma (± 0.042 Ma,
26 including the uncertainty in the age of Mes4Ts), respectively (assuming negligible
27 differential ^{39}Ar recoil loss). This age is within uncertainty of most recent astronomical
28 intercalibrations, permitting calculation of inter-laboratory mean ages of 28.176 ± 0.010
29 (± 0.023) Ma and 28.179 ± 0.009 (± 0.042) Ma, respectively. As the astronomical age of the
30 A1 tuff is more precise than that of the Mes4 tuff, we recommend that the former value is
31 adopted as the astronomical age for FCTs. This age is consistent with available U-Pb zircon
32 age data, but remains distinctly older than recent astronomical ages of 28.10 and 28.150
33 Ma inferred from deep-sea Ocean Drilling Program sediments, indicating that further work
34 is required to align the astronomical tuning of terrestrial versus deep-sea sediments. Based
35 on previous R-values for the Alder Creek Rhyolite sanidine (ACRs) and Mount Dromedary
36 biotite (MD-2b) reference minerals, co-irradiated with FCTs, we calculate revised
37 astronomically calibrated ages of 1.18342 ± 0.00069 (± 0.009) Ma for ACRs and $99.323 \pm$
38 0.077 (± 0.33) Ma for MD-2b, the latter amended to 99.20 ± 0.01 (± 0.38) Ma to account for
39 relative recoil loss of $^{39}\text{Ar}_K$. [To further enhance the accuracy of \$^{40}\text{Ar}/^{39}\text{Ar}\$ ages, our study](#)
40 [also highlights the need to carefully control neutron fluence gradients and consider recoil](#)
41 [effects.](#)

42

43

44 *Keywords:* $^{40}\text{Ar}/^{39}\text{Ar}$ geochronology, reference minerals, Fish Canyon Tuff, Alder Creek
45 Rhyolite, Mount Dromedary

46

47

48 **1. Introduction**

49

50 The $^{40}\text{Ar}/^{39}\text{Ar}$ dating technique is a variation on the conventional K-Ar method and is based
51 on the natural decay of ^{40}K to ^{40}Ar , where ^{39}Ar is produced by fast neutron irradiation (see
52 Schaen et al., 2020 and references therein). The proportion of $^{39}\text{Ar}_\text{K}$ produced during
53 irradiation, is determined indirectly by co-irradiating reference minerals (also termed
54 fluence monitors) of known age. Because argon isotopic ratios are measured, $^{40}\text{Ar}/^{39}\text{Ar}$
55 ages can be determined very precisely, with new generation mass spectrometers capable of
56 precision levels $<0.05\%$ (e.g., Phillips and Matchan, 2013; Phillips et al., 2017).

57 Despite the broad applicability of the $^{40}\text{Ar}/^{39}\text{Ar}$ technique to a range of K-bearing
58 minerals across much of Earth history, the accuracy of the method remains limited by
59 relatively large uncertainties in the potassium decay constants and the ages of key reference
60 minerals (see Schaen et al., 2020 and references therein). Recent efforts to address these
61 issues have included optimization of the $^{40}\text{Ar}/^{39}\text{Ar}$ method relative to the U-Pb technique
62 (Renne et al., 2010, 2011) and calibration of reference minerals (e.g., Fish Canyon Tuff
63 sanidine) to the astronomical timescale (e.g., Kuiper et al., 2004, 2008; Rivera et al., 2011,
64 2013; Phillips et al., 2017, 2020a; Niespolo et al., 2017). The optimization approach of
65 Renne et al. (2010, 2011) appears to produce $^{40}\text{Ar}/^{39}\text{Ar}$ ages for Cenozoic samples that are
66 slightly older than generally accepted ages and may require further refinement (see Phillips
67 et al., 2017).

68 Two indirect approaches have been used to calibrate common $^{40}\text{Ar}/^{39}\text{Ar}$ reference
69 mineral ages to the astronomical timescale, as their host units have not been identified in
70 deep-sea sequences. The first approach involves calibration relative to astronomically
71 tuned deep-sea cores that contain well-defined geological markers (e.g. Danish Ash-17;
72 Knox, 1984) and/or geomagnetic polarity excursions, for which $^{40}\text{Ar}/^{39}\text{Ar}$ data are also
73 available (e.g., Westerhold et al., 2015; Channell et al. 2020). The second approach
74 involves $^{40}\text{Ar}/^{39}\text{Ar}$ analyses of reference minerals (e.g., Fish Canyon Tuff sanidine - FCTs)

75 relative to tuff layers interbedded within astronomically tuned, terrestrial marine
76 successions in the Mediterranean region, notably the A1 Tephra (A1T) in the Faneromeni
77 section of Crete (Kuiper et al., 2004; Rivera et al., 2011, 2013; Phillips et al., 2017;
78 Niespolo et al., 2017) and the Mes4 tuff in the Messâdit section, Morocco (Kuiper et al.,
79 2008; Niespolo et al., 2017). In this study, we employ the latter approach and revisit the
80 astronomical calibration of the age for the well-known Fish Canyon Tuff sanidine reference
81 mineral.

82 The ca. 28 Ma, Fish Canyon Tuff sanidine (FCTs) (Cebula et al., 1986) is the most
83 widely used $^{40}\text{Ar}/^{39}\text{Ar}$ reference mineral, due to its high potassium content, low
84 atmospheric contamination levels and superior $^{40}\text{Ar}^*/^{39}\text{Ar}$ data reproducibility (e.g., Renne
85 et al., 1998; Phillips et al., 2017). However, reported K-Ar and $^{40}\text{Ar}/^{39}\text{Ar}$ ages for FCTs
86 vary from 27.54 ± 0.29 Ma to 28.39 ± 0.19 Ma (2σ), a spread of $\sim 3\%$ (e.g., Cebula et al.,
87 1986; Renne et al., 1998, 2010, 2011; Lanphere and Baardsgard, 2001; Spell and
88 McDougall, 2003; Kuiper et al., 2008; Ganerod et al., 2011; Rivera et al., 2011; Hall, 2013;
89 Niespolo et al., 2017; Phillips et al., 2017). Astronomically calibrated ages for FCTs
90 relative to Mediterranean tuffs (A1T, Mes4) show a more restricted age range ($28.126 \pm$
91 $0.019 - 28.21 \pm 0.18$ Ma; 2σ ; Kuiper et al., 2004, 2008; Phillips et al., 2017), but still vary
92 by $\sim 0.3\%$, which is well above current analytical precision capability (Table 1).

93 The above FCTs ages are mostly younger than values estimated relative to
94 astronomically tuned ash beds and/or geomagnetic excursions identified in Ocean Drilling
95 Program (ODP) cores, which range from $\sim 27.89 - 28.15$ Ma (see Westerhold et al., 2015;
96 Channell et al. 2020). For example, Westerhold et al. (2015) calculated an age for FCTs of
97 28.10 Ma, based on $^{40}\text{Ar}/^{39}\text{Ar}$ results for Ash-17 sanidine co-irradiated with FCTs (Storey
98 et al., 2007). By correlating astronomical and $^{40}\text{Ar}/^{39}\text{Ar}$ ages for 16 geomagnetic
99 excursions, Channell et al. (2020) estimated an FTCs age of 28.15 Ma.

100 Here, we re-evaluate the astronomical calibration of the Fish Canyon Tuff sanidine
 101 (FCTs) in relation to sanidine from the astronomically tuned A1 Tephra (Faneromeni
 102 section, Crete; Kuiper et al., 2004; Rivera et al., 2011) and Mes4 tuff (Messâdit section,
 103 Morocco; Kuiper et al., 2008; Niespolo et al., 2017). To facilitate inter-laboratory
 104 comparisons that are independent of reference mineral ages and decay constants, we
 105 calculate R-values (see Renne et al., 1998) for FCTs relative to A1Ts and Mes4Ts, where:

$$106 \quad R_{A1Ts}^{FCTs} = \frac{(e^{\lambda t_{FCTs}} - 1)}{(e^{\lambda t_{A1Ts}} - 1)} = \frac{(^{40}Ar^*/^{39}Ar_K)_{FCTs}}{(^{40}Ar^*/^{39}Ar_K)_{A1Ts}}, \text{ and}$$

$$107 \quad R_{Mes4Ts}^{FCTs} = \frac{(e^{\lambda t_{FCTs}} - 1)}{(e^{\lambda t_{Mes4Ts}} - 1)} = \frac{(^{40}Ar^*/^{39}Ar_K)_{FCTs}}{(^{40}Ar^*/^{39}Ar_K)_{Mes4Ts}}$$

108 Our analyses yield R-value that are consistent with most previous studies and permit the
 109 calculation of a revised, high precision age for the Fish Canyon Tuff sanidine reference
 110 mineral. In turn the new FCTs age allows calculation of revised ages for two other key
 111 reference minerals, Alder Creek Rhyolite sanidine (ACRs) and Mount Dromedary biotite
 112 (MD2b).

113

114

115 **2. Samples**

116

117 *2.1. Faneromeni A1 tephra sanidine, Crete (A1Ts)*

118

119 The A1 dacite-rhyolite tephra is an ~3cm thick unit within the upper Faneromeni deep
 120 marine sedimentary sequence in Crete (Hilgen et al., 1997; Kuiper et al., 2004; Rivera et
 121 al., 2011). The A1T sanidine phenocrysts used in this study derive from the same sample
 122 analysed by Kuiper et al. (2004), Rivera et al. (2011) and Phillips et al. (2017).
 123 Astronomical tuning of the Faneromeni section produced an age of 6.941 ± 0.005 Ma for

124 the A1 ash layer (Hilgen et al., 1995; Kuiper et al., 2004), revised to 6.943 ± 0.005 Ma (2σ)
125 by Rivera et al. (2011).

126

127 2.2. Messâdit Mes4 tuff *sanidine, Morocco (Mes4Ts)*

128

129 The ~5m thick Mes4 ignimbrite is one of several tephra units interbedded with marine
130 sediments in the Messâdit section of the Melilla Basin, Morocco (Kuiper et al., 2008). The
131 Mes4T sanidine phenocrysts used in this study are from the same sample analysed by
132 Kuiper et al. (2008). Astronomical tuning of the Moroccan section gives an age of $6.791 \pm$
133 0.010 Ma (2σ) for the Mes4 tuff (van Assen et al., 2006; Kuiper et al., 2008).

134

135 2.3. *Fish Canyon tuff sanidine, Colorado (FCTs)*

136

137 The well-known Fish Canyon Tuff (FCT) occurs in southern Colorado and forms part of
138 the extensive San Juan Volcanic Field (e.g., Lipman et al., 1997). The tuff is described as
139 a phenocryst-rich dacite/rhyolite tuff or a quartz-latitude ignimbrite (Spell and McDougall,
140 2003) The FCT sample used in the current study derives from the same ‘USGS’ locality
141 sampled by Spell & McDougall (2003).

142

143 **3. Analytical Methods**

144

145 3.1. *Sample preparation and irradiation*

146

147 The A1T and Mes4T sanidine separates were prepared at the Vrije Universiteit,
148 Amsterdam, using standard mineral separation methods (Kuiper et al., 2004; Kuiper et al.,

149 2008). A1T sanidine grains ranged in size from 0.3 – 0.4 mm, with Mes4T sanidine grains
150 being 0.8 – 1.0 mm in size. FCT sanidine crystals (0.3 – 0.4 mm) were prepared using
151 methods described by Phillips and Matchan (2013). Transparent, inclusion-free sanidine
152 crystals, with minimal adhering glass or groundmass material were selected for irradiation.
153 All sanidine separates were ultrasonically cleaned with dilute (7%) hydrofluoric acid (~2
154 minutes) and washed thoroughly with de-ionised water and acetone.

155 To minimise neutron fluence gradients, small aliquots (<10 mg) of A1Ts + FCTs
156 and Mes4Ts + FCTs sanidine grains were wrapped together in aluminium foil envelopes
157 (~5 mm²; ~2-3 grains deep). The packets were placed in the centre of silica glass tubes and
158 irradiated in the U.S. Geological Survey's (USGS) TRIGA reactor or the CLICIT facility
159 at the Oregon State University TRIGA (OSTR) reactor (Supplementary Table 1).

160

161 3.2. ⁴⁰Ar/³⁹Ar analytical procedures

162

163 ⁴⁰Ar/³⁹Ar analyses were undertaken in the Noble Gas laboratory at the University of
164 Melbourne (UoM), using a multi-collector Thermo Fisher Scientific ARGUSVI mass
165 spectrometer linked to a stainless steel gas extraction/purification line and a Photon
166 Machines Fusions 10.6 CO₂ laser system (Phillips and Matchan, 2013). ⁴⁰Ar, ³⁹Ar and ³⁷Ar
167 isotopes were measured on Faraday detectors (H1, AX, L2) with low noise 1 x 10¹³ Ω
168 resistors. ³⁸Ar measurements were conducted on Faraday detector L1, with a low noise 1 x
169 10¹² Ω resistor. A Compact Discrete Dynode (CDD) detector was utilized for ³⁶Ar
170 measurements.

171 Air aliquots from an automated pipette system were analysed prior to sample
172 analyses to monitor mass discrimination and Faraday/CCD detector bias relative to an
173 atmospheric ⁴⁰Ar/³⁶Ar ratio of 298.56 ± 0.31 (Lee et al., 2006). Faraday detector bias was

174 monitored via peak-jumping analyses on mass 40. Interference correction values for all
175 irradiations, based on analyses of irradiated K-glass and CaF₂ samples in associated
176 (longer) irradiations, are summarized in Supplementary Table 2. Contributions from ³⁶Ar_{Cl}
177 were calculated using a ³⁶Cl/³⁸Cl production ratio of 257.8 ± 2.5 (Renne et al., 2008) and
178 the (³⁶Ar/³⁸Ar)_{Air} value of 5.3050 ± 0.0084 (Lee et al., 2006).

179 Following neutron irradiation, sanidine crystals were loaded into copper sample
180 holders and placed into the stainless steel sample chamber with a ZnS cover slip. The
181 extraction line was baked at ~100°C until extraction line ⁴⁰Ar rate-of-rise levels had
182 decreased to <1fA/min. Sample gas, introduced into the ARGUSVI mass spectrometer,
183 was equilibrated for 20s, followed by multi-collection analysis of the five argon isotopes.
184 Peak signals were regressed to time zero - the time of gas inlet into the mass spectrometer.
185 Line blanks, measured between 1 - 3 sample analyses (typically <1.5 fA for ⁴⁰Ar;
186 Supplementary Table 2), were subtracted from succeeding sample results.

187

188 3.3. ⁴⁰Ar/³⁹Ar data handling

189 In the current study, single crystal, total fusion, ⁴⁰Ar/³⁹Ar analyses were conducted
190 on all A1T, Mes4T and FCT sanidine grains. The ⁴⁰Ar/³⁹Ar data were initially filtered to
191 exclude analyses with low radiogenic ⁴⁰Ar* (<80%), elevated Ca/K ratios (>0.5) or high
192 associated blanks (> 2fA) (Supplementary Table 2). Following previous studies (Rivera et
193 al., 2011; Niespolo et al., 2017), the data were then filtered using a normalized median
194 absolute deviation (nMAD) value >3 (Powell et al., 2020). To evaluate the robustness of
195 this statistical approach, we also used nMAD >2.5 and >4 filters, and calculated robust
196 Tukey Biweight mean values (Hoaglin et al., 1983; Ludwig, 2012) (Table 2).

197 R-values for FCTs relative to A1Ts and Mes4Ts were determined from weighted
198 mean ⁴⁰Ar/³⁹Ar fusion results using the above methods (Table 2). As ³⁹Ar_K recoil loss data

199 (e.g. Hall, 2013) are unavailable for A1Ts and Mes4Ts, we assumed similar values to FCTs
200 (~0.18%; Hall, 2013), and no impact on R-values. FCTs ages were calculated relative to
201 the astronomical ages for A1Ts (Rivera et al., 2011) and Mes4Ts (Kuiper et al., 2008), the
202 atmospheric argon composition of Lee et al. (2006), and the decay constants recommended
203 by Min et al. (2000). Note that the choice of decay constants (e.g., Steiger and Jäger, 1997;
204 Renne et al., 2010, 2011; Carter et al., 2020) has negligible impact on calculated R-values
205 and ages. Unless otherwise stated, uncertainties associated with R-values and ages are
206 reported at the 2σ level and exclude uncertainties in the ages of A1Ts and Mes4Ts and
207 decay constants. Final FCTs ages are reported with both internal and external uncertainties
208 (i.e. including uncertainties in the ages of A1Ts and Mes4Ts).

209

210

211 **4. Results**

212

213 Single crystal laser fusion analyses were conducted on A1T, Mes4T and FCT sanidine
214 aliquots across multiple irradiation batches (Supplementary Table 2). Weighted mean
215 $^{40}\text{Ar}^*/^{39}\text{Ar}$ and R-values for each sample batch are tabulated in Table 2. $^{40}\text{Ar}^*/^{39}\text{Ar}$ and
216 Ca/K ratios are compared in Figs. 1 and 2.

217 Calculated Ca/K ratios for FCTs range from 0.01 to 0.04, with most values between
218 0.01 and 0.02 (Figs 1, 2). Aside from two feldspar crystals (UM#85) with elevated ratios
219 (Ca/K >4.3; Supplementary Table 2), A1Ts Ca/K values are broadly similar, ranging from
220 0.005 to 0.045, although most plot between 0.01 and 0.03 (Fig. 1). Mes4Ts crystals exhibit
221 a narrow range of Ca/K ratios from 0.028 to 0.036 (Fig. 2). [The variations in Ca/K ratios](#)
222 [are consistent with fractional crystallisation processes and the lack of any clear correlation](#)

223 with $^{40}\text{Ar}^*/^{39}\text{Ar}$ values suggests the absence of obvious megacrysts, xenocrysts or
224 antecrysts in the sample aliquots.

225 Weighted mean $^{40}\text{Ar}^*/^{39}\text{Ar}$ and R-values are relatively insensitive to the statistical
226 filter used (Table 2; Figs. 1, 2). For consistency with previous studies (e.g. Rivera et al.,
227 2011; Niespolo et al. (2017), we compare results based on the nMAD > 3 filter. Mean
228 $^{40}\text{Ar}^*/^{39}\text{Ar}$ ratios for most sample aliquots are characterised by MSWD values >1 (up to
229 2.6; Figs. 1, 2), analogous to the observations in Phillips et al. (2017). Possible causes of
230 the excess dispersion could include analytical aberrations (e.g. anomalous blanks), variable
231 neutron fluence gradients and/or geological factors (e.g. inherited or excess argon).
232 Reported neutron fluence gradients for the CLICIT facility average $\sim 0.05 - 0.1\% \text{ mm}^{-1}$
233 (Rutte et al., 2018) and could account for most of the observed dispersion about the mean
234 ($\sim 0.1\%$), although we cannot negate other analytical and geological factors operating at
235 this level.

236 R_{A1Ts}^{FCTS} -values, calculated for co-irradiated A1Ts and FCTs aliquots, are analogous
237 across the four irradiation batches (UM#75, UM#82, UM#85, UM#87), and range from
238 4.0857 ± 0.0037 (0.092%; 2σ) to 4.0804 ± 0.0027 (0.066%; 2σ), giving a weighted mean
239 value of 4.0817 ± 0.0017 (0.041%; 2σ). This equates to FCTs ages ranging from $28.202 \pm$
240 0.026 Ma to $28.166 \pm 0.020 \text{ Ma}$, giving a mean value of $28.175 \pm 0.012 \text{ Ma}$, relative to an
241 astronomically tuned age of $6.943 \pm 0.005 \text{ Ma}$ for the A1 tuff (Rivera et al., 2011). For
242 comparison, the robust Tukey Biweight mean R_{A1Ts}^{FCTS} -value is 4.0815 ± 0.0021 , yielding an
243 age of $28.174 \pm 0.015 \text{ Ma}$ (Table 2).

244 $^{40}\text{Ar}/^{39}\text{Ar}$ data from irradiation batches UM#89 and UM#92 yielded indistinguishable
245 R_{Mes4Ts}^{FCTS} -values for co-irradiated Mes4T and FCT sanidine aliquots, of 4.1727 ± 0.0019
246 (0.046%; 2σ) and 4.1745 ± 0.0024 (0.057%; 2σ), yielding a mean value of 4.1734 ± 0.0015
247 (0.036%; 2σ). This equates to FCTs ages of $28.172 \pm 0.013 \text{ Ma}$ and $28.183 \pm 0.016 \text{ Ma}$

248 and a mean value of 28.176 ± 0.010 Ma, relative to an age of 6.791 ± 0.005 Ma for the
249 Mes4 tuff (Kuiper et al., 2008). These results are indistinguishable from the Tukey
250 Biweight mean R_{A17s}^{FCTS} -value of 4.1737 ± 0.0018 and FCTs age of 28.178 ± 0.012 Ma (Table
251 2).

252

253

254 **5. Discussion**

255

256 R-values provide a useful approach for comparing $^{40}\text{Ar}/^{39}\text{Ar}$ results from multiple
257 irradiations and different laboratories. In this section, we first compare our results with
258 previous astrological inter-calibration studies, before evaluating the optimal
259 astronomically calibrated age for FCTs and other $^{40}\text{Ar}/^{39}\text{Ar}$ reference minerals.

260

261 *5.1 Comparison with previous astrochronological results*

262

263 R_{A17s}^{FCTS} -values determined in the current study are compared with those from previous
264 studies in Fig. 3. The average R_{A17s}^{FCTS} -value (4.0817 ± 0.0017) determined from this study
265 is within uncertainty of previous R-values measured by Kuiper et al. (2004), Rivera et al.
266 (2011) and Niespolo et al. (2017) (Fig. 3). The improved precision of the current results is
267 largely attributable to the higher precision capability of the ARGUSVI mass spectrometer
268 system, with uncertainties on individual FCTs $^{40}\text{Ar}^*/^{39}\text{Ar}$ ratios typically $<0.05\%$ (1σ),
269 compared to uncertainties $>0.2\%$ recorded in earlier studies (Rivera et al., 2011; Niespolo
270 et al., 2017).

271 The current R_{A17s}^{FCTS} -value is distinct ($\sim 0.15\%$ higher) from that reported by Phillips
272 et al. (2017); reasons for this discordance are unclear. Possible explanations include

273 undetected fluctuations in analytical conditions, minor extraneous argon in the larger A1Ts
274 crystals used in the earlier study and/or variations in neutron fluence, possibly exacerbated
275 by separation of co-irradiated A1Ts and FCTs crystals. Given neutron fluence gradients of
276 $\sim 0.05 - 0.1\% \text{ mm}^{-1}$ (Rutte et al., 2018), separation by $\sim 2 - 3 \text{ mm}$ would be sufficient to
277 account for the above difference. Instrumental bias is considered unlikely, because R_{FCTs}^{ACRs} -
278 values (where ACRs is the well-known Alder Creek Rhyolite sanidine reference mineral)
279 reported by Phillips et al. (2017) are indistinguishable from those reported by Niespolo et
280 al. (2017) and Rivera et al. (2013).

281 The mean R_{Mes4Ts}^{FCTs} -value (4.1734 ± 0.0015) from this study is within uncertainty
282 (2σ) of the values determined by Kuiper et al. (2008; at both the Berkeley Geochronology
283 Centre and Vrije Universiteit laboratories) and Niespolo et al. (2017). This comparison is
284 maintained regardless of whether sanidine analyses from all Messâdit tuffs are included in
285 the comparison (Fig. 1).

286 In combination, the new R_{A1Ts}^{FCTs} - and R_{Mes4Ts}^{FCTs} -values indicate good agreement
287 between the four $^{40}\text{Ar}/^{39}\text{Ar}$ laboratories for which relevant data are available, noting that
288 the earlier data from Kuiper et al. (2004, 2008) were not determined using modern multi-
289 collector mass spectrometers. These results give weighted mean, inter-laboratory R_{A1Ts}^{FCTs} -
290 and R_{Mes4Ts}^{FCTs} -values of 4.0819 ± 0.0014 (0.034%) and 4.1738 ± 0.0013 (0.030%),
291 respectively.

292

293 *5.2 Astronomically calibrated age for FCTs*

294

295 The above R-values can be used to calculate revised astronomically calibrated ages for
296 FCTs (Fig. 2). Relative to ages of $6.943 \pm 0.005 \text{ Ma}$ for A1Ts (Rivera et al., 2011) and
297 $6.791 \pm 0.010 \text{ Ma}$ for the Mes4 tuff (Kuiper et al., 2008), the current data equate to FCTs

298 ages of 28.175 ± 0.012 Ma (2σ ; ± 0.023 Ma including the uncertainty in the age of A1Ts)
299 and 28.176 ± 0.010 Ma (2σ ; ± 0.042 Ma including the uncertainty in the age of Mes4Ts)
300 (Fig. 2).

301 The improved agreement in measured R-values (R_{A1Ts}^{FCTs} , R_{Mes4Ts}^{FCTs}) across multiple
302 irradiations and $^{40}\text{Ar}/^{39}\text{Ar}$ laboratories also permits determination of a revised
303 astronomically calibrated, inter-laboratory age for FCTs (Fig. 4). We calculate an inter-
304 laboratory weighted mean FCTs age of 28.176 ± 0.010 (± 0.023) Ma, including external
305 uncertainties) relative to the age of A1Ts, and an age of 28.179 ± 0.009 Ma (± 0.042) Ma,
306 including external uncertainties) relative to the astronomical age of Mes4Ts. Consideration
307 of all Messâdit sanidine results reported by Kuiper et al. (2008) yields an analogous mean
308 age of 28.181 ± 0.020 Ma (± 0.046 Ma) (Fig. 4).

309 Although the above astronomically calibrated FCTs ages are indistinguishable, the
310 astronomical age assigned to A1Ts is more precise than that of Mes4Ts. Consequently, we
311 recommend that the interlaboratory, astronomically calibrated mean value of $28.176 \pm$
312 0.010 (± 0.023) Ma be adopted as the age of the FCTs fluence monitor.

313 The above age is within uncertainty of the $^{206}\text{Pb}/^{238}\text{U}$ age of 28.196 ± 0.038 Ma
314 reported for FCT zircons by Wotzlaw et al. (2013), but numerically distinct from FCTs
315 ages of 28.10 Ma (Westerhold et al., 2015) and 28.150 Ma (Channell et al., 2020) inferred
316 from recent deep-sea core data, although no uncertainties are reported. Using the $^{40}\text{Ar}/^{39}\text{Ar}$
317 data documented for Ash-17 by Storey et al. (2007) and an uncertainty of 50 ka in
318 astronomical tuning (Westerhold et al. 2015), we calculate an FCTs age of 28.10 ± 0.04
319 Ma (2σ ; internal uncertainties). The FCTs age of 28.150 Ma reported by Channell et al.
320 (2020) is based on the minimum offset between the astronomical and $^{40}\text{Ar}/^{39}\text{Ar}$ ages for 16
321 geomagnetic excursions with no uncertainty assigned. Both these ages remain distinct from

322 our preferred age of 28.176 ± 0.011 Ma for FCTs. Clearly, further studies of astronomically
323 tuned ODP sections containing ash-beds amenable to $^{40}\text{Ar}/^{39}\text{Ar}$ dating are needed.

324

325 *5.2 Revised astronomically calibrated ages for Alder Creek Rhyolite sanidine (ACRs) and*
326 *Mount Dromedary biotite (MD-2)*

327

328 In addition to FCTs, other widely utilized reference minerals include the ca.1.18 Ma Alder
329 Creek Rhyolite sanidine (ACRs) (e.g., Turrin et al., 1994) and the ca.99.1 Ma Mount
330 Dromedary biotite (GA-1550 and MD-2) (e.g., McDougall and Wellman, 2011; Phillips et
331 al., 2017).

332 The Alder Creek Rhyolite is located on Cobb Mountain, Sonoma County,
333 California and forms part of the Clear Lake Volcanic Field (e.g., Mankinen et al., 1978;
334 Turrin et al., 1994). The ACR is characterised by transitional geomagnetic polarity and is
335 considered to record the geomagnetic reversal as the top of the Cobb Mountain Normal
336 Polarity subchron (e.g., Singer, 2014). Previous attempts to date the ACR are summarized
337 in Schaen et al. (2020). Based on the mean R_{FCTs}^{ACRs} -value of 0.041692 ± 0.000024 (0.058%)
338 reported by Phillips et al. (2017, 2020), and assuming negligible relative $^{39}\text{Ar}_K$ recoil loss,
339 we calculate an age of 1.18342 ± 0.00069 Ma (± 0.0090 Ma, including external
340 uncertainties) for the Alder Creek Rhyolite, compared to an FCTs age of 28.176 ± 0.010 Ma.
341 The above R_{FCTs}^{ACRs} -value is within uncertainty of the interlaboratory mean of $0.041715 \pm$
342 0.000029 (0.069%) reported by Schaen et al. (2020), noting that this value includes the
343 Phillips et al. (2017, 2020) data. This equates to an ACRs age of 1.18403 ± 0.00082
344 (± 0.011) Ma (relative to an FCTs age of 28.176 ± 0.010 Ma).

345 The Mount Dromedary igneous complex is located in New South Wales, Australia
346 (e.g., Boesen and Joplin, 1972; Smith et al., 1988). The GA-1550 (see McDougall and

347 Wellman, 2011) and MD-2 (Phillips et al., 2017) biotite samples were collected from the
348 same outer monzonite unit of the complex. Previous geochronological studies of the Mount
349 Dromedary complex are summarised by Phillips et al. (2017). Using the R_{FCTs}^{MD2b} -value of
350 3.5948 ± 0.0028 (2σ) from the latter study, we calculate a revised astronomically calibrated
351 age for MD-2 biotite (MD2b) of 99.323 ± 0.077 Ma (± 0.33 Ma, including external
352 uncertainties). This equates to a recoil affected age of 99.20 ± 0.01 (± 0.38) Ma, using $^{39}\text{Ar}_K$
353 recoil loss levels reported by Hall et al. (2013). Both ages are within uncertainty of the
354 $^{238}\text{U}/^{206}\text{Pb}$ zircon age of 99.12 ± 0.14 Ma obtained by Schoene et al. (2006).

355

356

357 **6. Conclusions**

358

359 $^{40}\text{Ar}/^{39}\text{Ar}$ analyses of Fish Canyon Tuff sanidine (FCTs) crystals, co-irradiated with A1
360 Tephra sanidine (A1Ts) and Mes4 Tuff sanidine (Mes4Ts) yield a mean R_{A1Ts}^{FCTs} -value of
361 4.0817 ± 0.0017 and a mean R_{Mes4Ts}^{FCTs} -value of 4.1734 ± 0.0015 , equating to FCTs ages of
362 28.175 ± 0.012 (± 0.023) Ma and 28.176 ± 0.010 (± 0.042) Ma, respectively, relative to
363 astronomically tuned ages for A1Ts (Rivera et al., 2011) and Mes4Ts (Kuiper et al., 2008).
364 These R-values and ages are consistent with most previously reported FCTs ages calibrated
365 against A1Ts and Mes4Ts, giving mean inter-laboratory ages of 28.176 ± 0.010 (± 0.023)
366 Ma and 28.179 ± 0.009 (± 0.042) Ma, respectively. It is recommended that the former age
367 be adopted as the astronomical age for FCTs. Using previous R-values for the Alder Creek
368 Rhyolite sanidine (ACRs) and Mount Dromedary biotite (MD2b) reference minerals co-
369 irradiated with FCTs, we calculate revised astronomically calibrated ages of $1.18342 \pm$
370 0.00069 (± 0.009) Ma and 99.323 ± 0.077 Ma (± 0.33) Ma, respectively, with the latter
371 corrected to 99.20 ± 0.01 (± 0.38) Ma to account for recoil loss of $^{39}\text{Ar}_K$.

372

373

374 **Acknowledgements**

375

376 This study is supported by AuScope and an Australian Research Council Discovery grant
377 (DP130100517) to DP and EM. S. Szczepanski is thanked for technical assistance in the
378 University of Melbourne $^{40}\text{Ar}/^{39}\text{Ar}$ laboratory. The manuscript has benefitted from formal
379 reviews by two anonymous reviewers and the editor, B. Kamber.

380

381

382 **References**

383

384 Boesen R.S., Joplin G.A., 1972. The form of the intrusive complex at Mount Dromedary,
385 New South Wales. *J. Geol. Soc. Aust.* 19, 345–349.

386 Carter, J., Ickert, R.B., Mark, D.F., Tremblay, M.M., Cresswell, A.J., Sanderson, D.C.W.,
387 2020. Production of ^{40}Ar by an overlooked mode of ^{40}K decay with implications for K-Ar
388 geochronology. *Geochron.* 2, 355-365.

389 Cebula G.T., Kunk M.J., Mehnert H.H., Naeser C.W., Obradovich J.D., Sutter, J.F., 1986.
390 The Fish Canyon Tuff, a potential standard for the ^{40}Ar – ^{39}Ar and fission-track dating
391 methods. *Terra Cognita* 6, 139–140.

392 Channell J.E.T., Singer B.S., Jicha B.R., 2020. Timing of Quaternary geomagnetic
393 reversals and excursions in volcanic and sedimentary archives. *Quat. Sci. Rev.* 228,
394 106114.

395 Ganerød, M., Chew, D.M., Smethurst, M.A., Troll, V.R., Corfu, F., Meade, F., Prestvik,
396 T., 2011. Geochronology of the Tardee Rhyolite Complex, Northern Ireland: Implications

397 of fission track studies, the North Atlantic Igneous Province and the age of the Fish Canyon
398 sanidine standard. *Chem. Geol.* 286, 222–228.

399 Hall C. M., 2013. Direct measurement of recoil effects on $^{40}\text{Ar}/^{39}\text{Ar}$ standards. In *Advances*
400 in $^{40}\text{Ar}/^{39}\text{Ar}$ Dating: from Archaeology to Planetary Sciences (eds. F. Jourdan, D.F. Mark
401 and C. Verati); *Geol. Soc. Lond. Spec. Publ.* 378.

402 Hilgen F.J., Krijgsman W., Wijbrans J.R., 1997. Direct comparison of astronomical and
403 $^{40}\text{Ar}/^{39}\text{Ar}$ ages of ash beds: potential implications for the age of mineral dating standards.
404 *Geophys. Res. Lett.* 24, 2043–2046.

405 Hoaglin D. C., Mosteller F. and Tukey J. W., 1983. *Understanding Robust and Exploratory*
406 *Data Analysis.* John Wiley and Sons, 345–349.

407 Knox, R. W. O. B., 1984. Nanoplankton zonation and the Palaeocene/Eocene boundary
408 beds of NW Europe: an indirect correlation by means of volcanic ash layers. *J. Geol. Soc.*
409 141, 993–999.

410 Kuiper K.F., Hilgen F.J., Steenbrink J., Wijbrans J.R., 2004. $^{40}\text{Ar}/^{39}\text{Ar}$ ages of tephras
411 intercalated in astronomically tuned Neogene sedimentary sequences in the eastern
412 Mediterranean. *Earth Planet. Sci. Lett.* 222, 583–597.

413 Kuiper K.F., Deino A., Hilgen F.J., Krijgsman W., Renne P.R., Wijbrans, J.R., 2008.
414 Synchronizing rock clocks of Earth history. *Science* 320, 500–504.

415 Lanphere M. A., Baadsgaard H., 2001. Precise K–Ar, $^{40}\text{Ar}/^{39}\text{Ar}$, Rb–Sr, U/Pb mineral ages
416 from the 27.5 Ma Fish Canyon Tuff reference standard. *Chem. Geol.* 175, 653–671.

417 Lee J.-Y., Marti K., Severinghaus J.P., Kawamura K., Yoo H.-S., Lee, J.B., Kim, J.S.,
418 2006. A redetermination of the isotopic abundances of atmospheric Ar. *Geochim.*
419 *Cosmochim. Acta* 70, 4507–4512.

420 Lipman P. W., Dungan M. A., Bachmann O., 1997. Comagmatic granophyric granite in
421 the Fish Canyon Tuff, Colorado: implications for magma-chamber processes during a large
422 ash-flow eruption. *Geology* 25, 915–918.

423 Ludwig K.R., 2012. User's Manual for Isoplot 3.75. A Geochronological Toolkit for
424 Microsoft Excel: Spec. Publ. No. 5, Berkeley Geochronology Center, Berkeley, California,
425 75 pp.

426 Mankinen E. A., Donnelly J. M., GrommeÅL C. S., 1978. Geomagnetic polarity event
427 recorded at 1.1 m.y. B.P. on Cobb Mountain, Clear Lake Volcanic field. *Calif. Geol.* 6,
428 653–656.

429 McDougall I., Wellman P., 2011. Calibration of GA1550 biotite standard for K/Ar and
430 $^{40}\text{Ar}/^{39}\text{Ar}$ dating. *Chem. Geol.* 280, 19–25.

431 Min, K.W., Mundil, R., Renne, P.R., Ludwig, K.R., 2000. A test for systematic errors in
432 $^{40}\text{Ar}/^{39}\text{Ar}$ geochronology through comparison with U/Pb analysis of a 1.1-Ga rhyolite.
433 *Geochim. Cosmochim. Acta* 64, 73-98.

434 Niespolo, E.M., Rutte, D., Deino, A.L., Renne, P.R., 2017. Intercalibration and age of the
435 Alder Creek sanidine $^{40}\text{Ar}/^{39}\text{Ar}$ standard. *Quat. Geochron.* 39, 205-213.

436 Phillips D., Matchan, E.L., 2013. Ultra-high precision $^{40}\text{Ar}/^{39}\text{Ar}$ ages for fish canyon tuff
437 and Alder Creek Rhyolite sanidine: new dating standards required? *Geochim. Cosmochim.*
438 *Acta*, 121, 229-239.

439 Phillips, D., Matchan, E.L., Honda, M., Kuiper, K.F., 2017. Astronomical calibration of
440 $^{40}\text{Ar}/^{39}\text{Ar}$ reference minerals using high-precision, multi-collector (ARGUSVI) mass
441 spectrometry. *Geochim. Cosmochim. Acta*, 196, 351-369.

442 Phillips, D., Matchan, E.L., Honda, M., Kuiper, K.F., 2020a. Corrigendum to
443 “Astronomical calibration of $^{40}\text{Ar}/^{39}\text{Ar}$ reference minerals using high-precision, multi-

444 collector (ARGUSVI) mass spectrometry”. [Geochim. Cosmochim. Acta 196 (2017) 351-
445 369]. Geochim. Cosmochim. Acta, 273, 406-410.

446 Phillips D., Matchan, E.L., 2020b. Corrigendum to “Ultra-high precision $^{40}\text{Ar}/^{39}\text{Ar}$ ages
447 for fish canyon tuff and Alder Creek Rhyolite sanidine: new dating standards required?”
448 [Geochim. Cosmochim. Acta 121 (2013) 229-239]. Geochim. Cosmochim. Acta, 273, 403-
449 405.

450 Powell, R., Green, E.C.R., Marillo Sialer, E., Woodhead, J., 2020. Robust isochron
451 calculation. Geochron. 2, 325-342.

452 Renne P.R., Swisher C.C., Deino A.L., Karner D.B., Owens T.L., DePaolo D.J., 1998.
453 Intercalibration of standards, absolute ages and uncertainties in $^{40}\text{Ar}/^{39}\text{Ar}$ dating. Chem.
454 Geol. 145, 117–152.

455 Renne P.R., Sharp Z.D., Heizler M.T., 2008. Cl-derived argon isotope production in the
456 CLICIT facility of OSTR reactor and the effects of the Cl-correction in $^{40}\text{Ar}/^{39}\text{Ar}$
457 geochronology. Chem. Geol. 255, 463-466.

458 Renne P.R., Mundil R., Balco G., Min K., Ludwig K.R., 2010. Joint determination of ^{40}K
459 decay constants and $^{40}\text{Ar}^*/^{40}\text{K}$ for the Fish Canyon sanidine standard, and improved
460 accuracy for $^{40}\text{Ar}/^{39}\text{Ar}$ geochronology. Geochim. Cosmochim. Acta 74, 5349–5367.

461 Renne P.R., Balco G., Ludwig K.R., Mundil R., Min K., 2011. Response to the comment
462 by W.H. Schwarz et al. on “Joint determination of ^{40}K decay constants and $^{40}\text{Ar}^*/^{40}\text{K}$ for
463 the Fish Canyon sanidine standard, and improved accuracy for $^{40}\text{Ar}/^{39}\text{Ar}$ geochronology”
464 by P.R. Renne et al., 2010. Geochim. Cosmochim. Acta 75, 5097–5100.

465 Rivera T.A., Storey M., Zeeden C., Hilgen F.J., Kuiper K., 2011. A refined astronomically
466 calibrated $^{40}\text{Ar}/^{39}\text{Ar}$ age for Fish Canyon sanidine. Earth Planet. Sci. Lett. 311, 420-426.

467 Rivera T.A., Storey M., Schmitz, M.D., Crowley, J.L., 2013. Age intercalibration of
468 $^{40}\text{Ar}/^{39}\text{Ar}$ sanidine and chemically distinct U/Pb zircon populations from the Alder Creek
469 Rhyolite Quaternary geochronology standard. *Chemical Geology* 345, 87-98.

470 Rutte, D., Becker, T.A., Deino, A.L., Reese, S.R., Renne, P.R., Schickler, R.A., 2018. The
471 new CLOCIT irradiation facility for $^{40}\text{Ar}/^{39}\text{Ar}$ geochronology: characterization,
472 comparison with CLICIT and implications for high-precision geochronology.
473 *Geostandards Geoanalytical Res.* 42 (3), 301-307.

474 Schaen, A.J., Jicha, B.R., Hodges, K.V., Vermeesch, P., Stelten, M.E., Mercer, C.M.,
475 Phillips, D., Rivera, T.A., Jourdan, F., Matchan, E.L., Hemming, S.R., Morgan, L.E.,
476 Kelley, S.P., Cassata, W.S., Heizler, M.T., Vasconcelos, P.M., Benowitz, J.A., Koppers,
477 A.A.P., Mark, D.F., Niespolo, E.M., Sprain, C.J., Hames, W.E., Kuiper, K.F., Turrin, B.D.,
478 Renne, P.R., Ross, J., Nomade, S., Guillou, H., Webb, L.E., Cohen, B.A., Calvert, A.T.,
479 Joyce, N., Ganerød, M., Wijbrans, J., Ishizuka, O., He, H., Ramirez, A., Pfänder, J.A.,
480 Lopez-Martínez, M., Qiu, H., Singer, B.S., 2021. Interpreting and reporting $^{40}\text{Ar}/^{39}\text{Ar}$
481 geochronologic data. *GSA Bulletin*, 133 (3-4): 461–487.

482 Schoene B., Crowley J. L., Condon D. J., Schmitz M. D., Bowring S. A., 2006. Reassessing
483 the uranium decay constants for geochronology using ID-TIMS U–Pb data. *Geochim.*
484 *Cosmochim. Acta* 70, 426–445.

485 Smith I. E. M., White A. J. R., Chappell B. W., Eggleton R. A., 1988. Fractionation in a
486 zoned monzonite pluton: Mount Dromedary, southeastern Australia. *Geol. Mag.* 125, 273–
487 284.

488 Spell, T.L. and McDougall, I., 2003. Characterization and calibration of $^{40}\text{Ar}/^{39}\text{Ar}$ dating
489 standards. *Chem. Geol.* 198, 189-211.

490 Steiger R.H., Jäger E., 1977. Subcommittee on geochronology: convention on the use of
491 decay constants in geo- and cosmochronology. *Earth Planet. Sci. Lett.* 36, 359-362.

492 Singer B. S., 2014. A Quaternary Geomagnetic Instability Time Scale. *Quat. Geochron.*
493 21, 29-52.

494 Storey, M., Duncan, R. A., Swisher, C. C., III, 2007. Paleocene-Eocene Thermal Maximum
495 and the Opening of the Northeast Atlantic, *Science*, 316, 587–589.

496 Turrin B. D., Donnely-Nolan J. M., Hearn B. C., 1994. $^{40}\text{Ar}/^{39}\text{Ar}$ ages from the rhyolite of
497 Alder Creek, California: age of the Cobb Mountain normal-polarity subchron revisited.
498 *Geology* 22, 251–254.

499 Van Assen, E., Kuiper, K.F., Barhoun, N., Krijgsman, W., Sierro, F.J., 2006. Messinian
500 astrochronology of the Melilla Basin: Stepwise restriction of the Mediterranean–Atlantic
501 connection through Morocco. *Paleogeog. Paleoclimat. Paleoecol.* 238, 15-31.

502 Westerhold T., Röhl U., Frederichs, S., Bohaty, S.M., Zachos J.C., 2015. Astronomical
503 calibration of the geological timescale: closing the middle Eocene gap. *Clim. Past*, 11,
504 1181-1195.

505 Wotzlaw J.-F., Schaltegger U., Frick D. A., Dungan M. A., Gerdes A. and Gunther D.,
506 2013. Tracking the evolution of largevolume silicic magma reservoirs from assembly to
507 supereruption. *Geology* 41(8), 867–870.

508

509

510 **Figure Captions**

511 Figure 1. $^{40}\text{Ar}/^{39}\text{Ar}^*$ and Ca/K ratios for Fish Canyon Tuff sanidine versus A1 Tuff
512 sanidine. Weighted mean $^{40}\text{Ar}/^{39}\text{Ar}^*$ values calculated using Isoplot (Ludwig, 2012).
513 Open symbols represent analyses excluded from the weighted mean $^{40}\text{Ar}/^{39}\text{Ar}^*$ ratio
514 based on nMAD >3 filtering.

515

516 Figure 2. $^{40}\text{Ar}/^{39}\text{Ar}^*$ and Ca/K ratios for Fish Canyon Tuff sanidine versus Mes4 Tuff
517 sanidine. Weighted mean $^{40}\text{Ar}/^{39}\text{Ar}^*$ values calculated using Isoplot (Ludwig, 2012). Open
518 symbols represent analyses excluded from the weighted mean $^{40}\text{Ar}/^{39}\text{Ar}^*$ ratio based on
519 nMAD >3 filtering.

520

521 **Fig. 3.** R_{A1Ts}^{FCTs} and R_{Mes4Ts}^{FCTs} values from previous work and the current study. Filled symbols
522 indicate R-values included in the inter-laboratory weighted mean calculations; open
523 symbols indicate R-values excluded from these calculations (see text for details).
524 Horizontal grey bars represent 2σ uncertainties in weighted mean R-values. BGC =
525 Berkeley Geochronology Centre; VU = Vrije Universiteit; QL = Quaternary Dating
526 Laboratory, Roskilde University; UoM = University of Melbourne.

527

528 **Fig. 4.** FCT sanidine $^{40}\text{Ar}/^{39}\text{Ar}$ ages from the current study compared with results from
529 previous work. FCTs ages are calculated relative to the astronomically tuned ages for A1Ts
530 (Kuiper et al., 2004; Rivera et al., 2011) and Mes4Ts (Kuiper et al., 2008). Filled symbols
531 indicate age values included in the inter-laboratory weighted mean calculations. Open
532 symbols indicate values excluded from these calculations (see text for details). Horizontal
533 grey bars represent 2σ uncertainties in weighted mean ages. Values in brackets include
534 uncertainties in the ages of A1Ts or Mes4Ts. Abbreviations as per figure 1.

1 Revised astronomically calibrated $^{40}\text{Ar}/^{39}\text{Ar}$ ages for the Fish
2 Canyon Tuff sanidine – closing the interlaboratory gap

3

4 D. Phillips^{a*}, E.L. Matchan^a, H. Dalton^a and Kuiper, K.F.^b

5 *^aSchool of Geography, Earth and Atmospheric Sciences, The University of Melbourne,*
6 *Parkville, VIC, 3010, Australia.*

7 *^bFaculty of Earth and Life Sciences, Vrije Universiteit Amsterdam, The Netherlands.*

8

9 *Corresponding author; E-mail: dphillip@unimelb.edu.au

10

11 **Abstract**

12

13 The $^{40}\text{Ar}/^{39}\text{Ar}$ geochronology method is capable of high precision (<0.05%), but remains
14 limited by relatively large uncertainties in ^{40}K decay constants and the ages of natural
15 reference mineral standards. The most widely used $^{40}\text{Ar}/^{39}\text{Ar}$ reference mineral is the well-
16 known ca. 28 Ma Fish Canyon Tuff sanidine (FCTs). Several studies have attempted to
17 calibrate FCTs against astronomically tuned tephra in Crete (Faneromeni A1 tephra) and
18 Morocco (Messâdit Mes4 tuff) as well as deep-sea sedimentary sequences. Previously
19 reported astronomically tuned ages range from 28.126 ± 0.019 to 28.21 ± 0.18 Ma (2σ), a
20 range of ~0.3%, compared to precision levels of <0.05% achievable by new generation,
21 multi-collector mass spectrometer systems. In this study, we revisit the astronomical
22 calibration of FCTs. Relative to ages of 6.943 ± 0.005 Ma for A1 tuff sanidine (A1Ts) and
23 6.791 ± 0.010 Ma (2σ) for Mes4 tuff sanidine (Mes4Ts), we calculate revised
24 astronomically tuned ages for Fish Canyon Tuff sanidine of 28.175 ± 0.012 Ma (± 0.023

25 Ma, including the uncertainty in the age of A1Ts) and 28.176 ± 0.010 Ma (± 0.042 Ma,
26 including the uncertainty in the age of Mes4Ts), respectively (assuming negligible
27 differential ^{39}Ar recoil loss). This age is within uncertainty of most recent astronomical
28 intercalibrations, permitting calculation of inter-laboratory mean ages of 28.176 ± 0.010
29 (± 0.023) Ma and 28.179 ± 0.009 (± 0.042) Ma, respectively. As the astronomical age of the
30 A1 tuff is more precise than that of the Mes4 tuff, we recommend that the former value is
31 adopted as the astronomical age for FCTs. This age is consistent with available U-Pb zircon
32 age data, but remains distinctly older than recent astronomical ages of 28.10 and 28.150
33 Ma inferred from deep-sea Ocean Drilling Program sediments, indicating that further work
34 is required to align the astronomical tuning of terrestrial versus deep-sea sediments. Based
35 on previous R-values for the Alder Creek Rhyolite sanidine (ACRs) and Mount Dromedary
36 biotite (MD-2b) reference minerals, co-irradiated with FCTs, we calculate revised
37 astronomically calibrated ages of 1.18342 ± 0.00069 (± 0.009) Ma for ACRs and $99.323 \pm$
38 0.077 (± 0.33) Ma for MD-2b, the latter amended to 99.20 ± 0.01 (± 0.38) Ma to account for
39 relative recoil loss of $^{39}\text{Ar}_K$. To further enhance the accuracy of $^{40}\text{Ar}/^{39}\text{Ar}$ ages, our study
40 also highlights the need to carefully control neutron fluence gradients and consider recoil
41 effects.

42

43

44 *Keywords:* $^{40}\text{Ar}/^{39}\text{Ar}$ geochronology, reference minerals, Fish Canyon Tuff, Alder Creek
45 Rhyolite, Mount Dromedary

46

47

48 **1. Introduction**

49

50 The $^{40}\text{Ar}/^{39}\text{Ar}$ dating technique is a variation on the conventional K-Ar method and is based
51 on the natural decay of ^{40}K to ^{40}Ar , where ^{39}Ar is produced by fast neutron irradiation (see
52 Schaen et al., 2020 and references therein). The proportion of $^{39}\text{Ar}_\text{K}$ produced during
53 irradiation, is determined indirectly by co-irradiating reference minerals (also termed
54 fluence monitors) of known age. Because argon isotopic ratios are measured, $^{40}\text{Ar}/^{39}\text{Ar}$
55 ages can be determined very precisely, with new generation mass spectrometers capable of
56 precision levels $<0.05\%$ (e.g., Phillips and Matchan, 2013; Phillips et al., 2017).

57 Despite the broad applicability of the $^{40}\text{Ar}/^{39}\text{Ar}$ technique to a range of K-bearing
58 minerals across much of Earth history, the accuracy of the method remains limited by
59 relatively large uncertainties in the potassium decay constants and the ages of key reference
60 minerals (see Schaen et al., 2020 and references therein). Recent efforts to address these
61 issues have included optimization of the $^{40}\text{Ar}/^{39}\text{Ar}$ method relative to the U-Pb technique
62 (Renne et al., 2010, 2011) and calibration of reference minerals (e.g., Fish Canyon Tuff
63 sanidine) to the astronomical timescale (e.g., Kuiper et al., 2004, 2008; Rivera et al., 2011,
64 2013; Phillips et al., 2017, 2020a; Niespolo et al., 2017). The optimization approach of
65 Renne et al. (2010, 2011) appears to produce $^{40}\text{Ar}/^{39}\text{Ar}$ ages for Cenozoic samples that are
66 slightly older than generally accepted ages and may require further refinement (see Phillips
67 et al., 2017).

68 Two indirect approaches have been used to calibrate common $^{40}\text{Ar}/^{39}\text{Ar}$ reference
69 mineral ages to the astronomical timescale, as their host units have not been identified in
70 deep-sea sequences. The first approach involves calibration relative to astronomically
71 tuned deep-sea cores that contain well-defined geological markers (e.g. Danish Ash-17;
72 Knox, 1984) and/or geomagnetic polarity excursions, for which $^{40}\text{Ar}/^{39}\text{Ar}$ data are also
73 available (e.g., Westerhold et al., 2015; Channell et al. 2020). The second approach
74 involves $^{40}\text{Ar}/^{39}\text{Ar}$ analyses of reference minerals (e.g., Fish Canyon Tuff sanidine - FCTs)

75 relative to tuff layers interbedded within astronomically tuned, terrestrial marine
76 successions in the Mediterranean region, notably the A1 Tephra (A1T) in the Faneromeni
77 section of Crete (Kuiper et al., 2004; Rivera et al., 2011, 2013; Phillips et al., 2017;
78 Niespolo et al., 2017) and the Mes4 tuff in the Messâdit section, Morocco (Kuiper et al.,
79 2008; Niespolo et al., 2017). In this study, we employ the latter approach and revisit the
80 astronomical calibration of the age for the well-known Fish Canyon Tuff sanidine reference
81 mineral.

82 The ca. 28 Ma, Fish Canyon Tuff sanidine (FCTs) (Cebula et al., 1986) is the most
83 widely used $^{40}\text{Ar}/^{39}\text{Ar}$ reference mineral, due to its high potassium content, low
84 atmospheric contamination levels and superior $^{40}\text{Ar}^*/^{39}\text{Ar}$ data reproducibility (e.g., Renne
85 et al., 1998; Phillips et al., 2017). However, reported K-Ar and $^{40}\text{Ar}/^{39}\text{Ar}$ ages for FCTs
86 vary from 27.54 ± 0.29 Ma to 28.39 ± 0.19 Ma (2σ), a spread of $\sim 3\%$ (e.g., Cebula et al.,
87 1986; Renne et al., 1998, 2010, 2011; Lanphere and Baardsgard, 2001; Spell and
88 McDougall, 2003; Kuiper et al., 2008; Ganerod et al., 2011; Rivera et al., 2011; Hall, 2013;
89 Niespolo et al., 2017; Phillips et al., 2017). Astronomically calibrated ages for FCTs
90 relative to Mediterranean tuffs (A1T, Mes4) show a more restricted age range ($28.126 \pm$
91 $0.019 - 28.21 \pm 0.18$ Ma; 2σ ; Kuiper et al., 2004, 2008; Phillips et al., 2017), but still vary
92 by $\sim 0.3\%$, which is well above current analytical precision capability (Table 1).

93 The above FCTs ages are mostly younger than values estimated relative to
94 astronomically tuned ash beds and/or geomagnetic excursions identified in Ocean Drilling
95 Program (ODP) cores, which range from $\sim 27.89 - 28.15$ Ma (see Westerhold et al., 2015;
96 Channell et al. 2020). For example, Westerhold et al. (2015) calculated an age for FCTs of
97 28.10 Ma, based on $^{40}\text{Ar}/^{39}\text{Ar}$ results for Ash-17 sanidine co-irradiated with FCTs (Storey
98 et al., 2007). By correlating astronomical and $^{40}\text{Ar}/^{39}\text{Ar}$ ages for 16 geomagnetic
99 excursions, Channell et al. (2020) estimated an FTCs age of 28.15 Ma.

100 Here, we re-evaluate the astronomical calibration of the Fish Canyon Tuff sanidine
 101 (FCTs) in relation to sanidine from the astronomically tuned A1 Tephra (Faneromeni
 102 section, Crete; Kuiper et al., 2004; Rivera et al., 2011) and Mes4 tuff (Messâdit section,
 103 Morocco; Kuiper et al., 2008; Niespolo et al., 2017). To facilitate inter-laboratory
 104 comparisons that are independent of reference mineral ages and decay constants, we
 105 calculate R-values (see Renne et al., 1998) for FCTs relative to A1Ts and Mes4Ts, where:

$$106 \quad R_{A1Ts}^{FCTs} = \frac{(e^{\lambda t_{FCTs}} - 1)}{(e^{\lambda t_{A1Ts}} - 1)} = \frac{(^{40}Ar^*/^{39}Ar_K)_{FCTs}}{(^{40}Ar^*/^{39}Ar_K)_{A1Ts}}, \text{ and}$$

$$107 \quad R_{Mes4Ts}^{FCTs} = \frac{(e^{\lambda t_{FCTs}} - 1)}{(e^{\lambda t_{Mes4Ts}} - 1)} = \frac{(^{40}Ar^*/^{39}Ar_K)_{FCTs}}{(^{40}Ar^*/^{39}Ar_K)_{Mes4Ts}}$$

108 Our analyses yield R-value that are consistent with most previous studies and permit the
 109 calculation of a revised, high precision age for the Fish Canyon Tuff sanidine reference
 110 mineral. In turn the new FCTs age allows calculation of revised ages for two other key
 111 reference minerals, Alder Creek Rhyolite sanidine (ACRs) and Mount Dromedary biotite
 112 (MD2b).

113

114

115 **2. Samples**

116

117 *2.1. Faneromeni A1 tephra sanidine, Crete (A1Ts)*

118

119 The A1 dacite-rhyolite tephra is an ~3cm thick unit within the upper Faneromeni deep
 120 marine sedimentary sequence in Crete (Hilgen et al., 1997; Kuiper et al., 2004; Rivera et
 121 al., 2011). The A1T sanidine phenocrysts used in this study derive from the same sample
 122 analysed by Kuiper et al. (2004), Rivera et al. (2011) and Phillips et al. (2017).
 123 Astronomical tuning of the Faneromeni section produced an age of 6.941 ± 0.005 Ma for

124 the A1 ash layer (Hilgen et al., 1995; Kuiper et al., 2004), revised to 6.943 ± 0.005 Ma (2σ)
125 by Rivera et al. (2011).

126

127 2.2. Messâdit Mes4 tuff *sanidine, Morocco (Mes4Ts)*

128

129 The ~5m thick Mes4 ignimbrite is one of several tephra units interbedded with marine
130 sediments in the Messâdit section of the Melilla Basin, Morocco (Kuiper et al., 2008). The
131 Mes4T sanidine phenocrysts used in this study are from the same sample analysed by
132 Kuiper et al. (2008). Astronomical tuning of the Moroccan section gives an age of $6.791 \pm$
133 0.010 Ma (2σ) for the Mes4 tuff (van Assen et al., 2006; Kuiper et al., 2008).

134

135 2.3. *Fish Canyon tuff sanidine, Colorado (FCTs)*

136

137 The well-known Fish Canyon Tuff (FCT) occurs in southern Colorado and forms part of
138 the extensive San Juan Volcanic Field (e.g., Lipman et al., 1997). The tuff is described as
139 a phenocryst-rich dacite/rhyolite tuff or a quartz-latitude ignimbrite (Spell and McDougall,
140 2003) The FCT sample used in the current study derives from the same 'USGS' locality
141 sampled by Spell & McDougall (2003).

142

143 **3. Analytical Methods**

144

145 3.1. *Sample preparation and irradiation*

146

147 The A1T and Mes4T sanidine separates were prepared at the Vrije Universiteit,
148 Amsterdam, using standard mineral separation methods (Kuiper et al., 2004; Kuiper et al.,

149 2008). A1T sanidine grains ranged in size from 0.3 – 0.4 mm, with Mes4T sanidine grains
150 being 0.8 – 1.0 mm in size. FCT sanidine crystals (0.3 – 0.4 mm) were prepared using
151 methods described by Phillips and Matchan (2013). Transparent, inclusion-free sanidine
152 crystals, with minimal adhering glass or groundmass material were selected for irradiation.
153 All sanidine separates were ultrasonically cleaned with dilute (7%) hydrofluoric acid (~2
154 minutes) and washed thoroughly with de-ionised water and acetone.

155 To minimise neutron fluence gradients, small aliquots (<10 mg) of A1Ts + FCTs
156 and Mes4Ts + FCTs sanidine grains were wrapped together in aluminium foil envelopes
157 (~5 mm²; ~2-3 grains deep). The packets were placed in the centre of silica glass tubes and
158 irradiated in the U.S. Geological Survey's (USGS) TRIGA reactor or the CLICIT facility
159 at the Oregon State University TRIGA (OSTR) reactor (Supplementary Table 1).

160

161 3.2. ⁴⁰Ar/³⁹Ar analytical procedures

162

163 ⁴⁰Ar/³⁹Ar analyses were undertaken in the Noble Gas laboratory at the University of
164 Melbourne (UoM), using a multi-collector Thermo Fisher Scientific ARGUSVI mass
165 spectrometer linked to a stainless steel gas extraction/purification line and a Photon
166 Machines Fusions 10.6 CO₂ laser system (Phillips and Matchan, 2013). ⁴⁰Ar, ³⁹Ar and ³⁷Ar
167 isotopes were measured on Faraday detectors (H1, AX, L2) with low noise 1 x 10¹³ Ω
168 resistors. ³⁸Ar measurements were conducted on Faraday detector L1, with a low noise 1 x
169 10¹² Ω resistor. A Compact Discrete Dynode (CDD) detector was utilized for ³⁶Ar
170 measurements.

171 Air aliquots from an automated pipette system were analysed prior to sample
172 analyses to monitor mass discrimination and Faraday/CCD detector bias relative to an
173 atmospheric ⁴⁰Ar/³⁶Ar ratio of 298.56 ± 0.31 (Lee et al., 2006). Faraday detector bias was

174 monitored via peak-jumping analyses on mass 40. Interference correction values for all
175 irradiations, based on analyses of irradiated K-glass and CaF₂ samples in associated
176 (longer) irradiations, are summarized in Supplementary Table 2. Contributions from ³⁶Ar_{Cl}
177 were calculated using a ³⁶Cl/³⁸Cl production ratio of 257.8 ± 2.5 (Renne et al., 2008) and
178 the (³⁶Ar/³⁸Ar)_{Air} value of 5.3050 ± 0.0084 (Lee et al., 2006).

179 Following neutron irradiation, sanidine crystals were loaded into copper sample
180 holders and placed into the stainless steel sample chamber with a ZnS cover slip. The
181 extraction line was baked at ~100°C until extraction line ⁴⁰Ar rate-of-rise levels had
182 decreased to <1fA/min. Sample gas, introduced into the ARGUSVI mass spectrometer,
183 was equilibrated for 20s, followed by multi-collection analysis of the five argon isotopes.
184 Peak signals were regressed to time zero - the time of gas inlet into the mass spectrometer.
185 Line blanks, measured between 1 - 3 sample analyses (typically <1.5 fA for ⁴⁰Ar;
186 Supplementary Table 2), were subtracted from succeeding sample results.

187

188 3.3. ⁴⁰Ar/³⁹Ar data handling

189 In the current study, single crystal, total fusion, ⁴⁰Ar/³⁹Ar analyses were conducted
190 on all A1T, Mes4T and FCT sanidine grains. The ⁴⁰Ar/³⁹Ar data were initially filtered to
191 exclude analyses with low radiogenic ⁴⁰Ar* (<80%), elevated Ca/K ratios (>0.5) or high
192 associated blanks (> 2fA) (Supplementary Table 2). Following previous studies (Rivera et
193 al., 2011; Niespolo et al., 2017), the data were then filtered using a normalized median
194 absolute deviation (nMAD) value >3 (Powell et al., 2020). To evaluate the robustness of
195 this statistical approach, we also used nMAD >2.5 and >4 filters, and calculated robust
196 Tukey Biweight mean values (Hoaglin et al., 1983; Ludwig, 2012) (Table 2).

197 R-values for FCTs relative to A1Ts and Mes4Ts were determined from weighted
198 mean ⁴⁰Ar/³⁹Ar fusion results using the above methods (Table 2). As ³⁹Ar_K recoil loss data

199 (e.g. Hall, 2013) are unavailable for A1Ts and Mes4Ts, we assumed similar values to FCTs
200 (~0.18%; Hall, 2013), and no impact on R-values. FCTs ages were calculated relative to
201 the astronomical ages for A1Ts (Rivera et al., 2011) and Mes4Ts (Kuiper et al., 2008), the
202 atmospheric argon composition of Lee et al. (2006), and the decay constants recommended
203 by Min et al. (2000). Note that the choice of decay constants (e.g., Steiger and Jäger, 1997;
204 Renne et al., 2010, 2011; Carter et al., 2020) has negligible impact on calculated R-values
205 and ages. Unless otherwise stated, uncertainties associated with R-values and ages are
206 reported at the 2σ level and exclude uncertainties in the ages of A1Ts and Mes4Ts and
207 decay constants. Final FCTs ages are reported with both internal and external uncertainties
208 (i.e. including uncertainties in the ages of A1Ts and Mes4Ts).

209

210

211 **4. Results**

212

213 Single crystal laser fusion analyses were conducted on A1T, Mes4T and FCT sanidine
214 aliquots across multiple irradiation batches (Supplementary Table 2). Weighted mean
215 $^{40}\text{Ar}^*/^{39}\text{Ar}$ and R-values for each sample batch are tabulated in Table 2. $^{40}\text{Ar}^*/^{39}\text{Ar}$ and
216 Ca/K ratios are compared in Figs. 1 and 2.

217 Calculated Ca/K ratios for FCTs range from 0.01 to 0.04, with most values between
218 0.01 and 0.02 (Figs 1, 2). Aside from two feldspar crystals (UM#85) with elevated ratios
219 (Ca/K >4.3; Supplementary Table 2), A1Ts Ca/K values are broadly similar, ranging from
220 0.005 to 0.045, although most plot between 0.01 and 0.03 (Fig. 1). Mes4Ts crystals exhibit
221 a narrow range of Ca/K ratios from 0.028 to 0.036 (Fig. 2). The variations in Ca/K ratios
222 are consistent with fractional crystallisation processes and the lack of any clear correlation

223 with $^{40}\text{Ar}^*/^{39}\text{Ar}$ values suggests the absence of obvious megacrysts, xenocrysts or
224 antecrysts in the sample aliquots.

225 Weighted mean $^{40}\text{Ar}^*/^{39}\text{Ar}$ and R-values are relatively insensitive to the statistical
226 filter used (Table 2; Figs. 1, 2). For consistency with previous studies (e.g. Rivera et al.,
227 2011; Niespolo et al. (2017), we compare results based on the nMAD > 3 filter. Mean
228 $^{40}\text{Ar}^*/^{39}\text{Ar}$ ratios for most sample aliquots are characterised by MSWD values >1 (up to
229 2.6; Figs. 1, 2), analogous to the observations in Phillips et al. (2017). Possible causes of
230 the excess dispersion could include analytical aberrations (e.g. anomalous blanks), variable
231 neutron fluence gradients and/or geological factors (e.g. inherited or excess argon).
232 Reported neutron fluence gradients for the CLICIT facility average $\sim 0.05 - 0.1\% \text{ mm}^{-1}$
233 (Rutte et al., 2018) and could account for most of the observed dispersion about the mean
234 ($\sim 0.1\%$), although we cannot negate other analytical and geological factors operating at
235 this level.

236 R_{A1Ts}^{FCTS} -values, calculated for co-irradiated A1Ts and FCTs aliquots, are analogous
237 across the four irradiation batches (UM#75, UM#82, UM#85, UM#87), and range from
238 4.0857 ± 0.0037 (0.092%; 2σ) to 4.0804 ± 0.0027 (0.066%; 2σ), giving a weighted mean
239 value of 4.0817 ± 0.0017 (0.041%; 2σ). This equates to FCTs ages ranging from $28.202 \pm$
240 0.026 Ma to 28.166 ± 0.020 Ma, giving a mean value of 28.175 ± 0.012 Ma, relative to an
241 astronomically tuned age of 6.943 ± 0.005 Ma for the A1 tuff (Rivera et al., 2011). For
242 comparison, the robust Tukey Biweight mean R_{A1Ts}^{FCTS} -value is 4.0815 ± 0.0021 , yielding an
243 age of 28.174 ± 0.015 Ma (Table 2).

244 $^{40}\text{Ar}/^{39}\text{Ar}$ data from irradiation batches UM#89 and UM#92 yielded indistinguishable
245 R_{Mes4Ts}^{FCTS} -values for co-irradiated Mes4T and FCT sanidine aliquots, of 4.1727 ± 0.0019
246 (0.046%; 2σ) and 4.1745 ± 0.0024 (0.057%; 2σ), yielding a mean value of 4.1734 ± 0.0015
247 (0.036%; 2σ). This equates to FCTs ages of 28.172 ± 0.013 Ma and 28.183 ± 0.016 Ma

248 and a mean value of 28.176 ± 0.010 Ma, relative to an age of 6.791 ± 0.005 Ma for the
249 Mes4 tuff (Kuiper et al., 2008). These results are indistinguishable from the Tukey
250 Biweight mean R_{A17s}^{FCTS} -value of 4.1737 ± 0.0018 and FCTs age of 28.178 ± 0.012 Ma (Table
251 2).

252

253

254 **5. Discussion**

255

256 R-values provide a useful approach for comparing $^{40}\text{Ar}/^{39}\text{Ar}$ results from multiple
257 irradiations and different laboratories. In this section, we first compare our results with
258 previous astrological inter-calibration studies, before evaluating the optimal
259 astronomically calibrated age for FCTs and other $^{40}\text{Ar}/^{39}\text{Ar}$ reference minerals.

260

261 *5.1 Comparison with previous astrochronological results*

262

263 R_{A17s}^{FCTS} -values determined in the current study are compared with those from previous
264 studies in Fig. 3. The average R_{A17s}^{FCTS} -value (4.0817 ± 0.0017) determined from this study
265 is within uncertainty of previous R-values measured by Kuiper et al. (2004), Rivera et al.
266 (2011) and Niespolo et al. (2017) (Fig. 3). The improved precision of the current results is
267 largely attributable to the higher precision capability of the ARGUSVI mass spectrometer
268 system, with uncertainties on individual FCTs $^{40}\text{Ar}^*/^{39}\text{Ar}$ ratios typically $<0.05\%$ (1σ),
269 compared to uncertainties $>0.2\%$ recorded in earlier studies (Rivera et al., 2011; Niespolo
270 et al., 2017).

271 The current R_{A17s}^{FCTS} -value is distinct ($\sim 0.15\%$ higher) from that reported by Phillips
272 et al. (2017); reasons for this discordance are unclear. Possible explanations include

273 undetected fluctuations in analytical conditions, minor extraneous argon in the larger A1Ts
274 crystals used in the earlier study and/or variations in neutron fluence, possibly exacerbated
275 by separation of co-irradiated A1Ts and FCTs crystals. Given neutron fluence gradients of
276 $\sim 0.05 - 0.1\% \text{ mm}^{-1}$ (Rutte et al., 2018), separation by $\sim 2 - 3 \text{ mm}$ would be sufficient to
277 account for the above difference. Instrumental bias is considered unlikely, because R_{FCTs}^{ACRs} -
278 values (where ACRs is the well-known Alder Creek Rhyolite sanidine reference mineral)
279 reported by Phillips et al. (2017) are indistinguishable from those reported by Niespolo et
280 al. (2017) and Rivera et al. (2013).

281 The mean R_{Mes4Ts}^{FCTs} -value (4.1734 ± 0.0015) from this study is within uncertainty
282 (2σ) of the values determined by Kuiper et al. (2008; at both the Berkeley Geochronology
283 Centre and Vrije Universiteit laboratories) and Niespolo et al. (2017). This comparison is
284 maintained regardless of whether sanidine analyses from all Messâdit tuffs are included in
285 the comparison (Fig. 1).

286 In combination, the new R_{A1Ts}^{FCTs} - and R_{Mes4Ts}^{FCTs} -values indicate good agreement
287 between the four $^{40}\text{Ar}/^{39}\text{Ar}$ laboratories for which relevant data are available, noting that
288 the earlier data from Kuiper et al. (2004, 2008) were not determined using modern multi-
289 collector mass spectrometers. These results give weighted mean, inter-laboratory R_{A1Ts}^{FCTs} -
290 and R_{Mes4Ts}^{FCTs} -values of 4.0819 ± 0.0014 (0.034%) and 4.1738 ± 0.0013 (0.030%),
291 respectively.

292

293 *5.2 Astronomically calibrated age for FCTs*

294

295 The above R-values can be used to calculate revised astronomically calibrated ages for
296 FCTs (Fig. 2). Relative to ages of $6.943 \pm 0.005 \text{ Ma}$ for A1Ts (Rivera et al., 2011) and
297 $6.791 \pm 0.010 \text{ Ma}$ for the Mes4 tuff (Kuiper et al., 2008), the current data equate to FCTs

298 ages of 28.175 ± 0.012 Ma (2σ ; ± 0.023 Ma including the uncertainty in the age of A1Ts)
299 and 28.176 ± 0.010 Ma (2σ ; ± 0.042 Ma including the uncertainty in the age of Mes4Ts)
300 (Fig. 2).

301 The improved agreement in measured R-values (R_{A1Ts}^{FCTs} , R_{Mes4Ts}^{FCTs}) across multiple
302 irradiations and $^{40}\text{Ar}/^{39}\text{Ar}$ laboratories also permits determination of a revised
303 astronomically calibrated, inter-laboratory age for FCTs (Fig. 4). We calculate an inter-
304 laboratory weighted mean FCTs age of 28.176 ± 0.010 (± 0.023) Ma, including external
305 uncertainties) relative to the age of A1Ts, and an age of 28.179 ± 0.009 Ma (± 0.042) Ma,
306 including external uncertainties) relative to the astronomical age of Mes4Ts. Consideration
307 of all Messâdit sanidine results reported by Kuiper et al. (2008) yields an analogous mean
308 age of 28.181 ± 0.020 Ma (± 0.046 Ma) (Fig. 4).

309 Although the above astronomically calibrated FCTs ages are indistinguishable, the
310 astronomical age assigned to A1Ts is more precise than that of Mes4Ts. Consequently, we
311 recommend that the interlaboratory, astronomically calibrated mean value of $28.176 \pm$
312 0.010 (± 0.023) Ma be adopted as the age of the FCTs fluence monitor.

313 The above age is within uncertainty of the $^{206}\text{Pb}/^{238}\text{U}$ age of 28.196 ± 0.038 Ma
314 reported for FCT zircons by Wotzlaw et al. (2013), but numerically distinct from FCTs
315 ages of 28.10 Ma (Westerhold et al., 2015) and 28.150 Ma (Channell et al., 2020) inferred
316 from recent deep-sea core data, although no uncertainties are reported. Using the $^{40}\text{Ar}/^{39}\text{Ar}$
317 data documented for Ash-17 by Storey et al. (2007) and an uncertainty of 50 ka in
318 astronomical tuning (Westerhold et al. 2015), we calculate an FCTs age of 28.10 ± 0.04
319 Ma (2σ ; internal uncertainties). The FCTs age of 28.150 Ma reported by Channell et al.
320 (2020) is based on the minimum offset between the astronomical and $^{40}\text{Ar}/^{39}\text{Ar}$ ages for 16
321 geomagnetic excursions with no uncertainty assigned. Both these ages remain distinct from

322 our preferred age of 28.176 ± 0.011 Ma for FCTs. Clearly, further studies of astronomically
323 tuned ODP sections containing ash-beds amenable to $^{40}\text{Ar}/^{39}\text{Ar}$ dating are needed.

324

325 *5.2 Revised astronomically calibrated ages for Alder Creek Rhyolite sanidine (ACRs) and*
326 *Mount Dromedary biotite (MD-2)*

327

328 In addition to FCTs, other widely utilized reference minerals include the ca.1.18 Ma Alder
329 Creek Rhyolite sanidine (ACRs) (e.g., Turrin et al., 1994) and the ca.99.1 Ma Mount
330 Dromedary biotite (GA-1550 and MD-2) (e.g., McDougall and Wellman, 2011; Phillips et
331 al., 2017).

332 The Alder Creek Rhyolite is located on Cobb Mountain, Sonoma County,
333 California and forms part of the Clear Lake Volcanic Field (e.g., Mankinen et al., 1978;
334 Turrin et al., 1994). The ACR is characterised by transitional geomagnetic polarity and is
335 considered to record the geomagnetic reversal as the top of the Cobb Mountain Normal
336 Polarity subchron (e.g., Singer, 2014). Previous attempts to date the ACR are summarized
337 in Schaen et al. (2020). Based on the mean R_{FCTs}^{ACRs} -value of 0.041692 ± 0.000024 (0.058%)
338 reported by Phillips et al. (2017, 2020), and assuming negligible relative $^{39}\text{Ar}_K$ recoil loss,
339 we calculate an age of 1.18342 ± 0.00069 Ma (± 0.0090 Ma, including external
340 uncertainties) for the Alder Creek Rhyolite, compared to an FCTs age of 28.176 ± 0.010 Ma.
341 The above R_{FCTs}^{ACRs} -value is within uncertainty of the interlaboratory mean of $0.041715 \pm$
342 0.000029 (0.069%) reported by Schaen et al. (2020), noting that this value includes the
343 Phillips et al. (2017, 2020) data. This equates to an ACRs age of 1.18403 ± 0.00082
344 (± 0.011) Ma (relative to an FCTs age of 28.176 ± 0.010 Ma).

345 The Mount Dromedary igneous complex is located in New South Wales, Australia
346 (e.g., Boesen and Joplin, 1972; Smith et al., 1988). The GA-1550 (see McDougall and

347 Wellman, 2011) and MD-2 (Phillips et al., 2017) biotite samples were collected from the
348 same outer monzonite unit of the complex. Previous geochronological studies of the Mount
349 Dromedary complex are summarised by Phillips et al. (2017). Using the R_{FCTs}^{MD2b} -value of
350 3.5948 ± 0.0028 (2σ) from the latter study, we calculate a revised astronomically calibrated
351 age for MD-2 biotite (MD2b) of 99.323 ± 0.077 Ma (± 0.33 Ma, including external
352 uncertainties). This equates to a recoil affected age of 99.20 ± 0.01 (± 0.38) Ma, using $^{39}\text{Ar}_K$
353 recoil loss levels reported by Hall et al. (2013). Both ages are within uncertainty of the
354 $^{238}\text{U}/^{206}\text{Pb}$ zircon age of 99.12 ± 0.14 Ma obtained by Schoene et al. (2006).

355

356

357 **6. Conclusions**

358

359 $^{40}\text{Ar}/^{39}\text{Ar}$ analyses of Fish Canyon Tuff sanidine (FCTs) crystals, co-irradiated with A1
360 Tephra sanidine (A1Ts) and Mes4 Tuff sanidine (Mes4Ts) yield a mean R_{A1Ts}^{FCTs} -value of
361 4.0817 ± 0.0017 and a mean R_{Mes4Ts}^{FCTs} -value of 4.1734 ± 0.0015 , equating to FCTs ages of
362 28.175 ± 0.012 (± 0.023) Ma and 28.176 ± 0.010 (± 0.042) Ma, respectively, relative to
363 astronomically tuned ages for A1Ts (Rivera et al., 2011) and Mes4Ts (Kuiper et al., 2008).
364 These R-values and ages are consistent with most previously reported FCTs ages calibrated
365 against A1Ts and Mes4Ts, giving mean inter-laboratory ages of 28.176 ± 0.010 (± 0.023)
366 Ma and 28.179 ± 0.009 (± 0.042) Ma, respectively. It is recommended that the former age
367 be adopted as the astronomical age for FCTs. Using previous R-values for the Alder Creek
368 Rhyolite sanidine (ACRs) and Mount Dromedary biotite (MD2b) reference minerals co-
369 irradiated with FCTs, we calculate revised astronomically calibrated ages of $1.18342 \pm$
370 0.00069 (± 0.009) Ma and 99.323 ± 0.077 Ma (± 0.33) Ma, respectively, with the latter
371 corrected to 99.20 ± 0.01 (± 0.38) Ma to account for recoil loss of $^{39}\text{Ar}_K$.

372

373

374 **Acknowledgements**

375

376 This study is supported by AuScope and an Australian Research Council Discovery grant
377 (DP130100517) to DP and EM. S. Szczepanski is thanked for technical assistance in the
378 University of Melbourne $^{40}\text{Ar}/^{39}\text{Ar}$ laboratory. The manuscript has benefitted from formal
379 reviews by two anonymous reviewers and the editor, B. Kamber.

380

381

382 **References**

383

384 Boesen R.S., Joplin G.A., 1972. The form of the intrusive complex at Mount Dromedary,
385 New South Wales. *J. Geol. Soc. Aust.* 19, 345–349.

386 Carter, J., Ickert, R.B., Mark, D.F., Tremblay, M.M., Cresswell, A.J., Sanderson, D.C.W.,
387 2020. Production of ^{40}Ar by an overlooked mode of ^{40}K decay with implications for K-Ar
388 geochronology. *Geochron.* 2, 355-365.

389 Cebula G.T., Kunk M.J., Mehnert H.H., Naeser C.W., Obradovich J.D., Sutter, J.F., 1986.
390 The Fish Canyon Tuff, a potential standard for the ^{40}Ar – ^{39}Ar and fission-track dating
391 methods. *Terra Cognita* 6, 139–140.

392 Channell J.E.T., Singer B.S., Jicha B.R., 2020. Timing of Quaternary geomagnetic
393 reversals and excursions in volcanic and sedimentary archives. *Quat. Sci. Rev.* 228,
394 106114.

395 Ganerød, M., Chew, D.M., Smethurst, M.A., Troll, V.R., Corfu, F., Meade, F., Prestvik,
396 T., 2011. Geochronology of the Tardee Rhyolite Complex, Northern Ireland: Implications

397 of fission track studies, the North Atlantic Igneous Province and the age of the Fish Canyon
398 sanidine standard. *Chem. Geol.* 286, 222–228.

399 Hall C. M., 2013. Direct measurement of recoil effects on $^{40}\text{Ar}/^{39}\text{Ar}$ standards. In *Advances*
400 in $^{40}\text{Ar}/^{39}\text{Ar}$ Dating: from Archaeology to Planetary Sciences (eds. F. Jourdan, D.F. Mark
401 and C. Verati); *Geol. Soc. Lond. Spec. Publ.* 378.

402 Hilgen F.J., Krijgsman W., Wijbrans J.R., 1997. Direct comparison of astronomical and
403 $^{40}\text{Ar}/^{39}\text{Ar}$ ages of ash beds: potential implications for the age of mineral dating standards.
404 *Geophys. Res. Lett.* 24, 2043–2046.

405 Hoaglin D. C., Mosteller F. and Tukey J. W., 1983. *Understanding Robust and Exploratory*
406 *Data Analysis.* John Wiley and Sons, 345–349.

407 Knox, R. W. O. B., 1984. Nanoplankton zonation and the Palaeocene/Eocene boundary
408 beds of NW Europe: an indirect correlation by means of volcanic ash layers. *J. Geol. Soc.*
409 141, 993–999.

410 Kuiper K.F., Hilgen F.J., Steenbrink J., Wijbrans J.R., 2004. $^{40}\text{Ar}/^{39}\text{Ar}$ ages of tephras
411 intercalated in astronomically tuned Neogene sedimentary sequences in the eastern
412 Mediterranean. *Earth Planet. Sci. Lett.* 222, 583–597.

413 Kuiper K.F., Deino A., Hilgen F.J., Krijgsman W., Renne P.R., Wijbrans, J.R., 2008.
414 Synchronizing rock clocks of Earth history. *Science* 320, 500–504.

415 Lanphere M. A., Baadsgaard H., 2001. Precise K–Ar, $^{40}\text{Ar}/^{39}\text{Ar}$, Rb–Sr, U/Pb mineral ages
416 from the 27.5 Ma Fish Canyon Tuff reference standard. *Chem. Geol.* 175, 653–671.

417 Lee J.-Y., Marti K., Severinghaus J.P., Kawamura K., Yoo H.-S., Lee, J.B., Kim, J.S.,
418 2006. A redetermination of the isotopic abundances of atmospheric Ar. *Geochim.*
419 *Cosmochim. Acta* 70, 4507–4512.

420 Lipman P. W., Dungan M. A., Bachmann O., 1997. Comagmatic granophyric granite in
421 the Fish Canyon Tuff, Colorado: implications for magma-chamber processes during a large
422 ash-flow eruption. *Geology* 25, 915–918.

423 Ludwig K.R., 2012. User's Manual for Isoplot 3.75. A Geochronological Toolkit for
424 Microsoft Excel: Spec. Publ. No. 5, Berkeley Geochronology Center, Berkeley, California,
425 75 pp.

426 Mankinen E. A., Donnelly J. M., GrommeÅL C. S., 1978. Geomagnetic polarity event
427 recorded at 1.1 m.y. B.P. on Cobb Mountain, Clear Lake Volcanic field. *Calif. Geol.* 6,
428 653–656.

429 McDougall I., Wellman P., 2011. Calibration of GA1550 biotite standard for K/Ar and
430 $^{40}\text{Ar}/^{39}\text{Ar}$ dating. *Chem. Geol.* 280, 19–25.

431 Min, K.W., Mundil, R., Renne, P.R., Ludwig, K.R., 2000. A test for systematic errors in
432 $^{40}\text{Ar}/^{39}\text{Ar}$ geochronology through comparison with U/Pb analysis of a 1.1-Ga rhyolite.
433 *Geochim. Cosmochim. Acta* 64, 73-98.

434 Niespolo, E.M., Rutte, D., Deino, A.L., Renne, P.R., 2017. Intercalibration and age of the
435 Alder Creek sanidine $^{40}\text{Ar}/^{39}\text{Ar}$ standard. *Quat. Geochron.* 39, 205-213.

436 Phillips D., Matchan, E.L., 2013. Ultra-high precision $^{40}\text{Ar}/^{39}\text{Ar}$ ages for fish canyon tuff
437 and Alder Creek Rhyolite sanidine: new dating standards required? *Geochim. Cosmochim.*
438 *Acta*, 121, 229-239.

439 Phillips, D., Matchan, E.L., Honda, M., Kuiper, K.F., 2017. Astronomical calibration of
440 $^{40}\text{Ar}/^{39}\text{Ar}$ reference minerals using high-precision, multi-collector (ARGUSVI) mass
441 spectrometry. *Geochim. Cosmochim. Acta*, 196, 351-369.

442 Phillips, D., Matchan, E.L., Honda, M., Kuiper, K.F., 2020a. Corrigendum to
443 “Astronomical calibration of $^{40}\text{Ar}/^{39}\text{Ar}$ reference minerals using high-precision, multi-

444 collector (ARGUSVI) mass spectrometry”. [Geochim. Cosmochim. Acta 196 (2017) 351-
445 369]. Geochim. Cosmochim. Acta, 273, 406-410.

446 Phillips D., Matchan, E.L., 2020b. Corrigendum to “Ultra-high precision $^{40}\text{Ar}/^{39}\text{Ar}$ ages
447 for fish canyon tuff and Alder Creek Rhyolite sanidine: new dating standards required?”
448 [Geochim. Cosmochim. Acta 121 (2013) 229-239]. Geochim. Cosmochim. Acta, 273, 403-
449 405.

450 Powell, R., Green, E.C.R., Marillo Sialer, E., Woodhead, J., 2020. Robust isochron
451 calculation. Geochron. 2, 325-342.

452 Renne P.R., Swisher C.C., Deino A.L., Karner D.B., Owens T.L., DePaolo D.J., 1998.
453 Intercalibration of standards, absolute ages and uncertainties in $^{40}\text{Ar}/^{39}\text{Ar}$ dating. Chem.
454 Geol. 145, 117–152.

455 Renne P.R., Sharp Z.D., Heizler M.T., 2008. Cl-derived argon isotope production in the
456 CLICIT facility of OSTR reactor and the effects of the Cl-correction in $^{40}\text{Ar}/^{39}\text{Ar}$
457 geochronology. Chem. Geol. 255, 463-466.

458 Renne P.R., Mundil R., Balco G., Min K., Ludwig K.R., 2010. Joint determination of ^{40}K
459 decay constants and $^{40}\text{Ar}^*/^{40}\text{K}$ for the Fish Canyon sanidine standard, and improved
460 accuracy for $^{40}\text{Ar}/^{39}\text{Ar}$ geochronology. Geochim. Cosmochim. Acta 74, 5349–5367.

461 Renne P.R., Balco G., Ludwig K.R., Mundil R., Min K., 2011. Response to the comment
462 by W.H. Schwarz et al. on “Joint determination of ^{40}K decay constants and $^{40}\text{Ar}^*/^{40}\text{K}$ for
463 the Fish Canyon sanidine standard, and improved accuracy for $^{40}\text{Ar}/^{39}\text{Ar}$ geochronology”
464 by P.R. Renne et al., 2010. Geochim. Cosmochim. Acta 75, 5097–5100.

465 Rivera T.A., Storey M., Zeeden C., Hilgen F.J., Kuiper K., 2011. A refined astronomically
466 calibrated $^{40}\text{Ar}/^{39}\text{Ar}$ age for Fish Canyon sanidine. Earth Planet. Sci. Lett. 311, 420-426.

467 Rivera T.A., Storey M., Schmitz, M.D., Crowley, J.L., 2013. Age intercalibration of
468 $^{40}\text{Ar}/^{39}\text{Ar}$ sanidine and chemically distinct U/Pb zircon populations from the Alder Creek
469 Rhyolite Quaternary geochronology standard. *Chemical Geology* 345, 87-98.

470 Rutte, D., Becker, T.A., Deino, A.L., Reese, S.R., Renne, P.R., Schickler, R.A., 2018. The
471 new CLOCIT irradiation facility for $^{40}\text{Ar}/^{39}\text{Ar}$ geochronology: characterization,
472 comparison with CLICIT and implications for high-precision geochronology.
473 *Geostandards Geoanalytical Res.* 42 (3), 301-307.

474 Schaen, A.J., Jicha, B.R., Hodges, K.V., Vermeesch, P., Stelten, M.E., Mercer, C.M.,
475 Phillips, D., Rivera, T.A., Jourdan, F., Matchan, E.L., Hemming, S.R., Morgan, L.E.,
476 Kelley, S.P., Cassata, W.S., Heizler, M.T., Vasconcelos, P.M., Benowitz, J.A., Koppers,
477 A.A.P., Mark, D.F., Niespolo, E.M., Sprain, C.J., Hames, W.E., Kuiper, K.F., Turrin, B.D.,
478 Renne, P.R., Ross, J., Nomade, S., Guillou, H., Webb, L.E., Cohen, B.A., Calvert, A.T.,
479 Joyce, N., Ganerød, M., Wijbrans, J., Ishizuka, O., He, H., Ramirez, A., Pfänder, J.A.,
480 Lopez-Martínez, M., Qiu, H., Singer, B.S., 2021. Interpreting and reporting $^{40}\text{Ar}/^{39}\text{Ar}$
481 geochronologic data. *GSA Bulletin*, 133 (3-4): 461–487.

482 Schoene B., Crowley J. L., Condon D. J., Schmitz M. D., Bowring S. A., 2006. Reassessing
483 the uranium decay constants for geochronology using ID-TIMS U–Pb data. *Geochim.*
484 *Cosmochim. Acta* 70, 426–445.

485 Smith I. E. M., White A. J. R., Chappell B. W., Eggleton R. A., 1988. Fractionation in a
486 zoned monzonite pluton: Mount Dromedary, southeastern Australia. *Geol. Mag.* 125, 273–
487 284.

488 Spell, T.L. and McDougall, I., 2003. Characterization and calibration of $^{40}\text{Ar}/^{39}\text{Ar}$ dating
489 standards. *Chem. Geol.* 198, 189-211.

490 Steiger R.H., Jäger E., 1977. Subcommittee on geochronology: convention on the use of
491 decay constants in geo- and cosmochronology. *Earth Planet. Sci. Lett.* 36, 359-362.

492 Singer B. S., 2014. A Quaternary Geomagnetic Instability Time Scale. *Quat. Geochron.*
493 21, 29-52.

494 Storey, M., Duncan, R. A., Swisher, C. C., III, 2007. Paleocene-Eocene Thermal Maximum
495 and the Opening of the Northeast Atlantic, *Science*, 316, 587–589.

496 Turrin B. D., Donnely-Nolan J. M., Hearn B. C., 1994. $^{40}\text{Ar}/^{39}\text{Ar}$ ages from the rhyolite of
497 Alder Creek, California: age of the Cobb Mountain normal-polarity subchron revisited.
498 *Geology* 22, 251–254.

499 Van Assen, E., Kuiper, K.F., Barhoun, N., Krijgsman, W., Sierro, F.J., 2006. Messinian
500 astrochronology of the Melilla Basin: Stepwise restriction of the Mediterranean–Atlantic
501 connection through Morocco. *Paleogeog. Paleoclimat. Paleoecol.* 238, 15-31.

502 Westerhold T., Röhl U., Frederichs, S., Bohaty, S.M., Zachos J.C., 2015. Astronomical
503 calibration of the geological timescale: closing the middle Eocene gap. *Clim. Past*, 11,
504 1181-1195.

505 Wotzlaw J.-F., Schaltegger U., Frick D. A., Dungan M. A., Gerdes A. and Gunther D.,
506 2013. Tracking the evolution of largevolume silicic magma reservoirs from assembly to
507 supereruption. *Geology* 41(8), 867–870.

508

509

510 **Figure Captions**

511 Figure 1. $^{40}\text{Ar}/^{39}\text{Ar}^*$ and Ca/K ratios for Fish Canyon Tuff sanidine versus A1 Tuff
512 sanidine. Weighted mean $^{40}\text{Ar}/^{39}\text{Ar}^*$ values calculated using Isoplot (Ludwig, 2012).
513 Open symbols represent analyses excluded from the weighted mean $^{40}\text{Ar}/^{39}\text{Ar}^*$ ratio
514 based on nMAD >3 filtering.

515

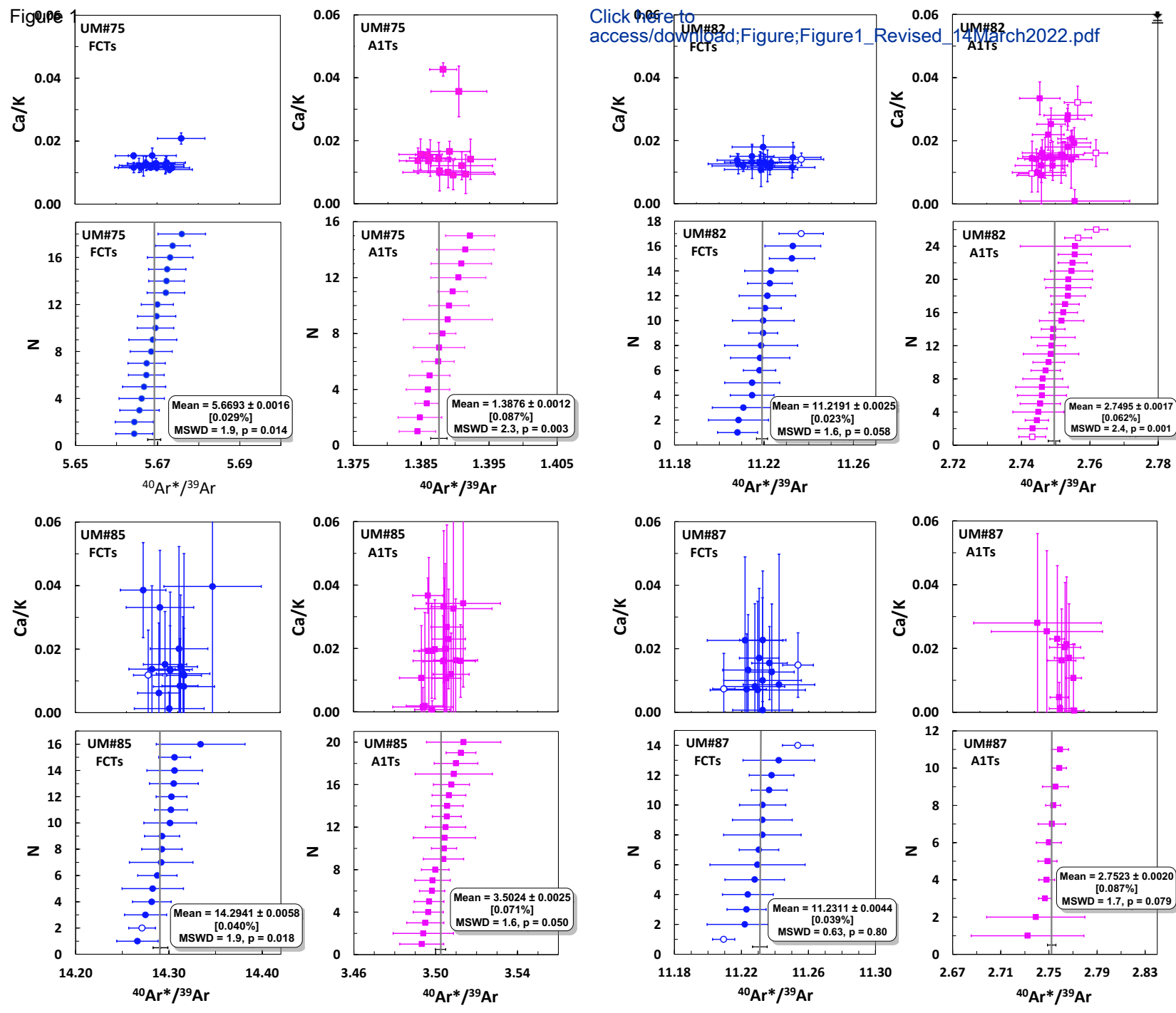
516 Figure 2. $^{40}\text{Ar}/^{39}\text{Ar}^*$ and Ca/K ratios for Fish Canyon Tuff sanidine versus Mes4 Tuff
517 sanidine. Weighted mean $^{40}\text{Ar}/^{39}\text{Ar}^*$ values calculated using Isoplot (Ludwig, 2012). Open
518 symbols represent analyses excluded from the weighted mean $^{40}\text{Ar}/^{39}\text{Ar}^*$ ratio based on
519 nMAD >3 filtering.

520

521 **Fig. 3.** R_{A1Ts}^{FCTs} and R_{Mes4Ts}^{FCTs} values from previous work and the current study. Filled symbols
522 indicate R-values included in the inter-laboratory weighted mean calculations; open
523 symbols indicate R-values excluded from these calculations (see text for details).
524 Horizontal grey bars represent 2σ uncertainties in weighted mean R-values. BGC =
525 Berkeley Geochronology Centre; VU = Vrije Universiteit; QL = Quaternary Dating
526 Laboratory, Roskilde University; UoM = University of Melbourne.

527

528 **Fig. 4.** FCT sanidine $^{40}\text{Ar}/^{39}\text{Ar}$ ages from the current study compared with results from
529 previous work. FCTs ages are calculated relative to the astronomically tuned ages for A1Ts
530 (Kuiper et al., 2004; Rivera et al., 2011) and Mes4Ts (Kuiper et al., 2008). Filled symbols
531 indicate age values included in the inter-laboratory weighted mean calculations. Open
532 symbols indicate values excluded from these calculations (see text for details). Horizontal
533 grey bars represent 2σ uncertainties in weighted mean ages. Values in brackets include
534 uncertainties in the ages of A1Ts or Mes4Ts. Abbreviations as per figure 1.



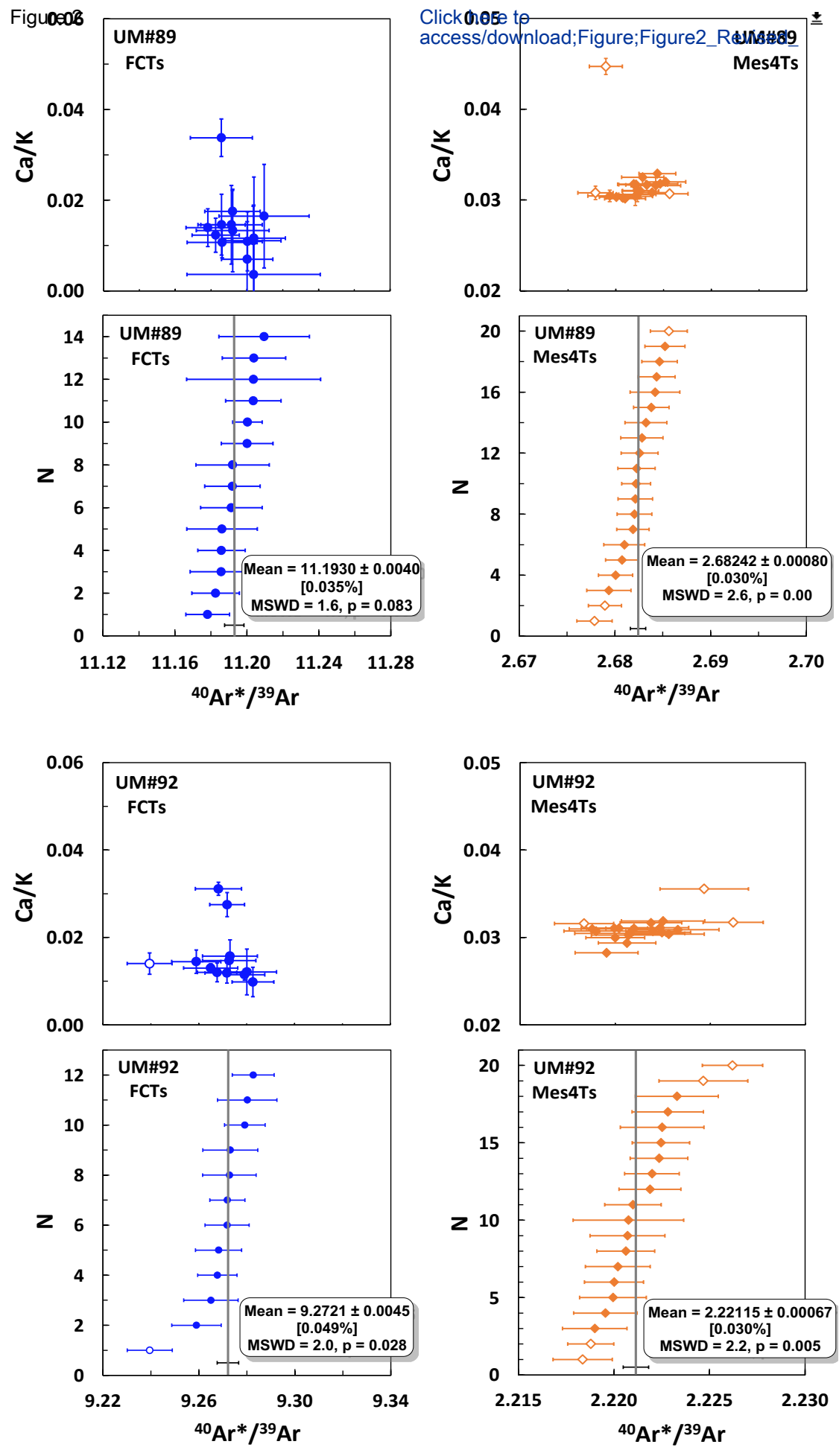


Figure 3

[Click here to access/download;Figure;Figure3_R](#)

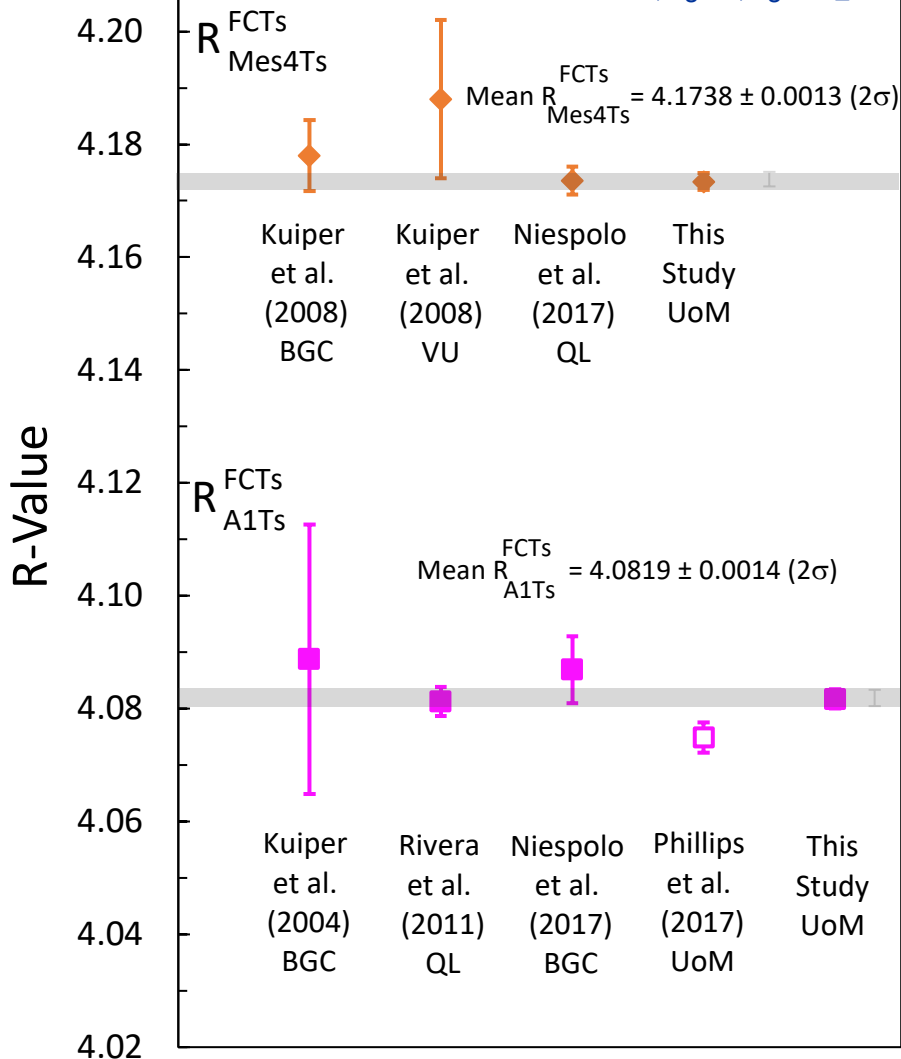


Figure 4

[Click here to access/download;Figure;Figure4_Revised.pdf](#)

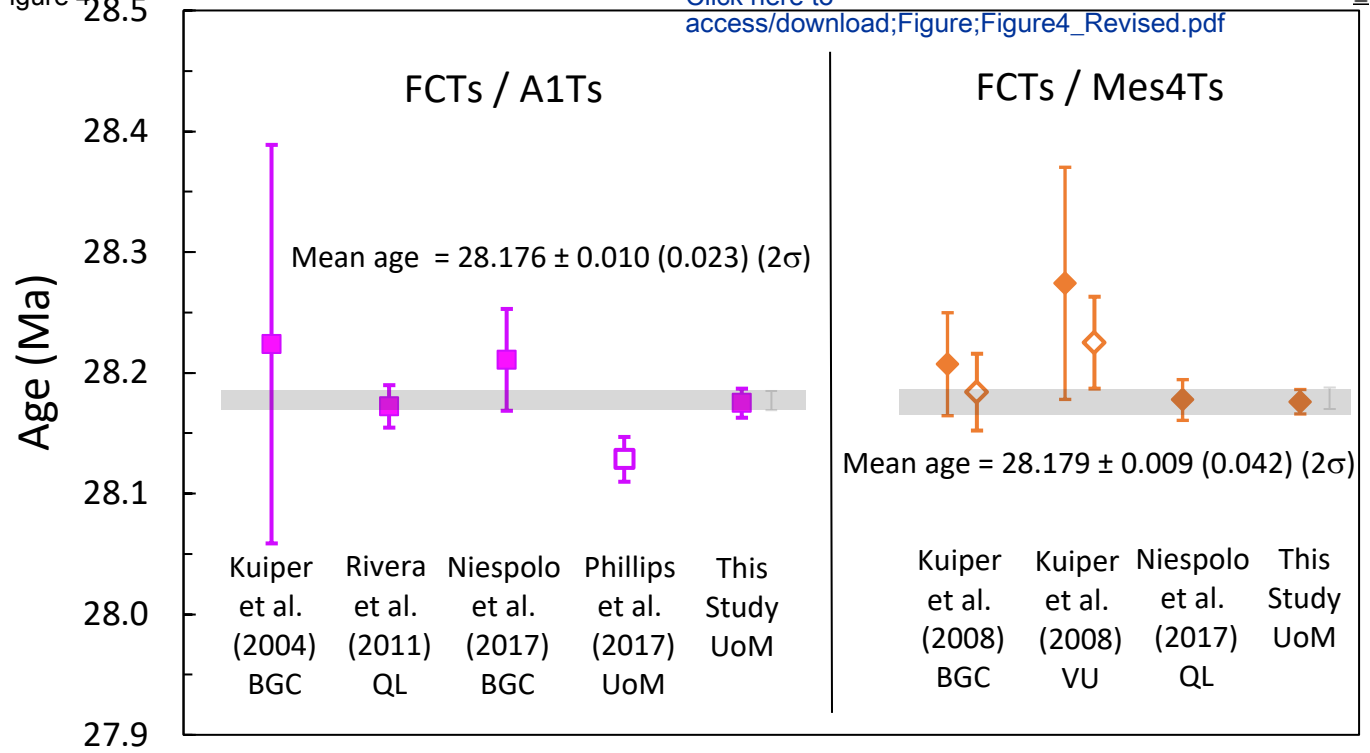


Table 1

Previously reported R-values and $^{40}\text{Ar}/^{39}\text{Ar}$ ages for Fish Canyon Tuff sanidine (FCTs) relative to the ages of the A1 Tephra sanidine (A1Ts) and Mes4 Tuff sanidine (Mes4Ts).

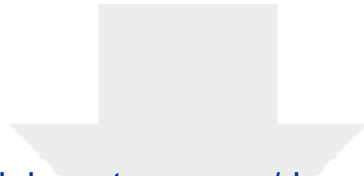
R-value ^{1,2}	$\pm 2\sigma$ (abs.)	$\pm 2\sigma$ (%)	FCTs age (Ma)	$\pm 2\sigma$ (abs.)	$\pm 2\sigma$ (%)	Reference
$R_{\text{FCTs/A1Ts}}^1$						
4.0888	0.0239	0.58	28.224	0.165	0.58	Kuiper et al. (2004)
4.0813	0.0026	0.06	28.172	0.018	0.06	Rivera et al. (2011)
4.0869	0.0059	0.15	28.211	0.042	0.15	Niespolo et al. (2017)
4.0749	0.0027	0.07	28.129	0.019	0.07	Phillips et al. (2017)
$R_{[\text{FCTs/Mes4}]}^2$						
4.1780	0.0063	0.15	28.207	0.043	0.15	Kuiper et al. (2008)
4.1736	0.0025	0.06	28.274	0.096	0.34	Niespolo et al. (2017)

¹ $R_{\text{FCTs/A1Ts}} = [^{40}\text{Ar}^*/^{39}\text{Ar}]_{\text{FCTs}} / [^{40}\text{Ar}^*/^{39}\text{Ar}]_{\text{A1Ts}}$

² $R_{[\text{FCTs/Mes4Ts}]} = [^{40}\text{Ar}^*/^{39}\text{Ar}]_{\text{FCTs}} / [^{40}\text{Ar}^*/^{39}\text{Ar}]_{\text{Mes4Ts}}$

Table 2.Weighted mean R-values and $^{40}\text{Ar}^*/^{39}\text{Ar}$ ages for FCT, A1T and Mes4 sanidine fusion analyses from irradiations in this study.

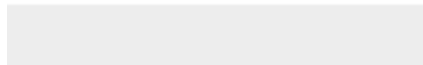
Irradiation No.	Sample	No. Grains	Wtd. Mean $^{40}\text{Ar}^*/^{39}\text{Ar}$ (NMAD >2.5)		Wtd. Mean $^{40}\text{Ar}^*/^{39}\text{Ar}$ (NMAD >3)		Wtd. Mean $^{40}\text{Ar}^*/^{39}\text{Ar}$ (NMAD >4)		Wtd. Mean $^{40}\text{Ar}^*/^{39}\text{Ar}$ (Tukey)		R-Value (nMAD >2.5)		R-Value (nMAD >3)		R-Value (nMAD >4)		R-Value* (Tukey)	
			$\pm 2\sigma$	$\pm 2\sigma$	$\pm 2\sigma$	$\pm 2\sigma$	$\pm 2\sigma$	$\pm 2\sigma$	$\pm 2\sigma$	$\pm 2\sigma$	$\pm 2\sigma$	$\pm 2\sigma$	$\pm 2\sigma$	$\pm 2\sigma$	$\pm 2\sigma$	$\pm 2\sigma$	$\pm 2\sigma$	$\pm 2\sigma$
UM#75	FCTs	18	5.6693	0.0016	5.6693	0.0016	5.6693	0.0016	5.6692	0.0017	4.0833	0.0037	4.0857	0.0037	4.0857	0.0037	4.0838	0.0043
	A1Ts	15	1.3884	0.0012	1.3876	0.0012	1.3876	0.0012	1.3882	0.0014								
UM#82	FCTs	17	11.2191	0.0027	11.2191	0.0025	11.2202	0.0039	11.2198	0.0042	4.0789	0.0025	4.0804	0.0027	4.0808	0.0030	4.0802	0.0032
	A1Ts	26	2.7505	0.0015	2.7495	0.0017	2.7495	0.0018	2.7498	0.0019								
UM#85	FCTs	16	14.2941	0.0058	14.2941	0.0058	14.2909	0.0079	14.2932	0.0087	4.0812	0.0034	4.0812	0.0034	4.0803	0.0037	4.0809	0.0043
	A1Ts	21	3.5024	0.0026	3.5024	0.0026	3.5024	0.0026	3.5025	0.0030								
UM#87	FCTs	14	11.2311	0.0044	11.2311	0.0044	11.2311	0.0044	11.2309	0.0057	4.0806	0.0039	4.0806	0.0039	4.0806	0.0039	4.0841	0.0080
	A1Ts	11	2.7523	0.0024	2.7523	0.0024	2.7523	0.0024	2.7499	0.0053								
Mean (n = 4)											4.0806	0.0016	4.0817	0.0017	4.0818	0.0018	4.0815	0.0021
FCTs Age (Ma)											28.168	0.011	28.175	0.012	28.176	0.012	28.174	0.015
UM#89	FCTs	15	11.1930	0.0040	11.1930	0.0040	11.1930	0.0040	11.1939	0.0058	4.1732	0.0019	4.1727	0.0019	4.1728	0.0020	4.1730	0.0026
	Mes4	20	2.68211	0.00074	2.68242	0.00080	2.68242	0.00080	2.68249	0.00094								
UM#92	FCTs	12	9.2721	0.0045	9.2721	0.0045	9.2721	0.0045	9.2720	0.0047	4.1745	0.0024	4.1745	0.0024	4.1750	0.0025	4.1745	0.0026
	Mes4	20	2.22115	0.00067	2.22115	0.00067	2.22084	0.00078	2.22108	0.00083								
Mean (n = 2)											4.1737	0.0015	4.1734	0.0015	4.1735	0.0015	4.1737	0.0018
FCTs Age (Ma)											28.178	0.010	28.176	0.010	28.177	0.010	28.178	0.012
R(A1Ts/Mes4)											0.97769	0.00052	0.97803	0.00054	0.97803	0.00056	0.97791	0.00066

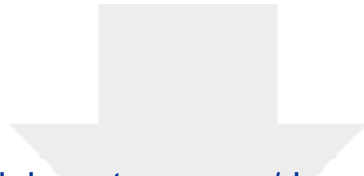


[Click here to access/download](#)

Supplementary file

Supplementary_Table1_Revised.xlsx

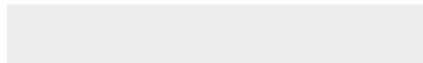




[Click here to access/download](#)

Supplementary file

Supplementary_Table2_Revised.xlsx



Declaration of interests

The authors declare that they have no known competing financial interests or personal relationships that could have appeared to influence the work reported in this paper.

The authors declare the following financial interests/personal relationships which may be considered as potential competing interests: